

APR 10 1946

NATIONAL ADVISORY COMMITTEE FOR AERONAUTICS



TECHNICAL NOTE

No. 1044

EFFECT OF MACH AND REYNOLDS NUMBERS
ON MAXIMUM LIFT COEFFICIENT

By John R. Spreiter and Paul J. Steffen

Ames Aeronautical Laboratory
Moffett Field, Calif.



Washington
March 1946

NACA LIBRARY
LANGLEY MEMORIAL AERONAUTICAL
LABORATORY
Langley Field, Va.

NATIONAL ADVISORY COMMITTEE FOR AERONAUTICS

TECHNICAL NOTE NO. 1044

EFFECT OF MACH AND REYNOLDS NUMBERS
ON MAXIMUM LIFT COEFFICIENT

By John R. Spreiter and Paul J. Steffen

SUMMARY

A compilation has been made of maximum-lift-coefficient data obtained in flight with six pursuit-type airplanes embodying typical conventional and low-drag airfoils. These flight data, which cover a range of Mach numbers from 0.15 to 0.72 and of Reynolds numbers from 4,400,000 to 19,500,000, have been analyzed together with pertinent model and airfoil data obtained in several wind tunnels.

It was found that the maximum lift coefficient varied with Mach number down to Mach numbers of approximately 0.15. When the effects of Mach number were considered, as well as those of Reynolds number, good correlation was found to exist between flight data and available wind tunnel data, providing buffeting or other factors did not prevent attainment of the actual maximum lift coefficient. The same considerations provided good agreement among limited airfoil data from various wind tunnels,

At subcritical Mach numbers, the maximum lift coefficient decreased steadily with increasing Mach number for all airplanes tested. The effects of Reynolds number were determined for three of the airplanes and found to be qualitatively as described in NACA Report No. 586; quantitatively, the effects of Reynolds number on the maximum lift coefficient decreased progressively with increasing Mach number, becoming nil at a Mach number of approximately 0.55. The critical Reynolds number increased nearly linearly with Mach number.

In the supercritical Mach number range, the maximum lift coefficient of conventional airfoils continued to diminish with increasing Mach number, while that of the low-drag airfoils reached a minimum at a Mach number between 0.40 and 0.55

and began increasing until secondary peak values were reached at a Mach number between 0.60 and 0.66. At supercritical Mach numbers, no effects of Reynolds numbers were apparent for two of the three airplanes on which pertinent data were obtained. On the third airplane the maximum lift coefficient was affected by Reynolds number but the phenomenon appeared to be basically different from that experienced at subcritical Mach numbers.

INTRODUCTION

A knowledge of the effects of Mach and Reynolds numbers on the maximum lift coefficient is becoming of greater importance as the speeds and altitudes attainable by modern airplanes continually increase. Since most maximum-lift tests conducted to date have been either at full-scale Reynolds numbers and low Mach numbers or at high Mach numbers and small Reynolds numbers, very little is known about the interrelated effects of these two parameters on the maximum lift coefficient. In order to obtain quantitative information on these effects, flight tests were conducted at Ames Aeronautical Laboratory on six airplanes, three having NACA conventional airfoil sections, two having NACA low-drag sections, and the sixth having a North American Aviation - NACA compromise low-drag section. The results of these tests which cover a range of Mach numbers from 0.15 to 0.72 and of Reynolds numbers from 4,400,000 to 19,500,000 are assembled together with a considerable quantity of pertinent wind-tunnel data, and analyzed in the present report. From this analysis, general conclusions have been reached indicating the manner in which the maximum lift coefficient is influenced by variations of Mach and Reynolds numbers.

DESCRIPTION OF AIRPLANES AND INSTRUMENTATION

To afford a variety of commonly used airfoil sections, and to permit correlation with existing wind-tunnel results, six particular pursuit-type airplanes were selected for the flight-test portion of this research. For convenience in the presentation of the test results and the following discussion, the type airplane and airplane model will be utilized rather than the airfoil designation when referring to specific results. The aircraft used in the conduct of the flight tests

were the Bell P-39N and P-63A airplanes, the Grumman F6F-3 airplane, the Lockheed P-38F and YP-80A airplanes, and the North American P-51B airplane. The P-38F, P-39N, and the F6F-3 are equipped with NACA conventional airfoils; the P-63A and YP-80A are provided with NACA low-drag airfoils, and the P-51B has a North American Aviation - NACA compromise low-drag airfoil. Two-view drawings of the test aircraft together with pertinent specifications are shown in figure 1. Photographs of the test airplanes are presented in figures 2(a) through 2(f), and wing-root and -tip airfoil sections for these airplanes are presented in figure 3.

The P-51B and the YP-80A airplanes had very carefully filled, waxed, and polished surfaces. The other airplanes were painted with standard camouflage paint. Of the six airplanes tested, the P-38F and P-39N airplanes had the roughest finish and the most openings in the wings.

Standard NACA photographically recording flight instruments were used to measure as a function of time the following variables: indicated airspeed, pressure altitude, normal acceleration, pitching and rolling velocities. The airspeed heads used for all the airplanes tested were of the freely swiveling type, to minimize errors due to the large angles of attack encountered in the tests, and with the exception of the P-38F airplane were mounted on booms extending approximately a chord length or more ahead of the leading edge near the wing tip. The airspeed head of the P-38F airplane was mounted on a boom extending ahead of the fuselage nose. The installations were calibrated for position error.

The free-air temperatures were obtained either from radiosonde observations or from readings of calibrated free-air-temperature indicators or recorders in the airplane.

Photographs of the 0.167-, 0.350-, and 0.333-scale models of the P-38, P-39N, and XP-80 airplanes, respectively, as tested in the Ames 16-foot high-speed wind tunnel are shown in figures 2(g), 2(h), and 2(i). As may be seen in these photographs, the XP-80 model was a complete model; the P-38 model was complete except for the propellers; and the P-39N model was complete except for the propeller and tail. The forces and moments were recorded by self-balancing, recording beam scales.

The airfoil tests conducted in the Ames 1- by 3 $\frac{1}{2}$ -foot high-speed wind tunnel were of 6-inch-chord metal models mounted so as to span completely the 1-foot width of the

tunnel test section. The lift was obtained either from integration of pressure distributions over the airfoils or from measurements of the reactions on the tunnel walls of the forces experienced by the airfoils.

TEST PROCEDURE

All flight data in this report were obtained in gradual stalls made during turns or pull-ups with the airplanes in the clean condition (flaps and landing gear up). With the five propeller-driven airplanes, all stalls were made with the engine throttled and the propeller in the high-pitch setting. Although the power was on during the stalls of the jet-propelled YP-80A airplane, the data were considered similar to the power-off condition of the propeller-driven airplanes as no slipstream existed over the wing.

The flight maximum lift coefficients were calculated by the following formula:

$$C_{L_{\max}} = \frac{WA_Z}{qS}$$

where

$C_{L_{\max}}$ maximum lift coefficient

W weight of the airplane at the time of stall, pounds

A_Z normal acceleration factor, the ratio of the net aerodynamic force along the airplane Z-axis at the stall (positive when directed upward), to the weight of the airplane

S wing area, including area extending through the fuselage and nacelles, square feet

q dynamic pressure, pounds per square foot

An error of less than two percent was caused by the assumption in the preceding formula that the lift was equal to the normal force WA_Z .

Throughout this report, the Reynolds number was computed

using the mean aerodynamic chord as the characteristic length.

The maximum lift coefficient obtainable in flight may be limited by the effects resulting from a localized stall over a limited portion of the wing or from distortion of the lift curve by compressibility effects; these may be manifested by unstable motions of the airplane, by loss of control effectiveness, or by buffeting of the airplane or controls. Since the extent of such a stall may not be sufficient to prevent attaining higher lift coefficients at greater angles of attack in the wind tunnel, a difference between the maximum lift coefficient obtainable in flight tests and in wind-tunnel tests will usually be anticipated. The characteristics assumed to indicate the stall for each of the six airplanes tested are summarized in the following table:

<u>Airplane</u>	<u>Low Mach numbers</u>	<u>High Mach numbers</u>
F6F-3	Roll-off and slight buffeting	Moderate buffeting with pitch-down, followed by porpoising motions
P-38F	Slight buffeting	Buffeting. Pilot reported apparent ineffectiveness of elevators to increase lift coefficient
P-39N	Buffeting and roll-off	Buffeting and pitch-down
P-51B	Buffeting and roll-off	Severe buffeting with mild roll-off
P-63A	Roll-off and pitch-down	Abrupt roll-off
YP-80A	Roll-off with slight buffeting	Slight buffeting

At low Mach numbers, it is shown that the stalls of all the airplanes except the P-38F were characterized by roll-off. Since stalls characterized by roll-off are clearly defined by the motions of the airplane, the maximum lift coefficients obtained in flight are relatively independent of piloting technique and the amount of control available, and would probably be similar to the values measured in a wind tunnel. At high Mach numbers, however, the stalls of only two airplanes were characterized by roll-off, those of the remaining airplanes

being characterized by buffeting accompanied, in some cases, by pitching motions. Maximum lift coefficients defined by buffeting are probably less than the actual maximum lift coefficient by amounts that are a function of what the pilot considers tolerable buffeting limits. It should be noted that the maximum-lift-coefficient data shown in this report were repeatable even when determined by buffeting considerations indicating that the flight values have significance as the maximum usable lift coefficient of the airplane. A further discussion of this phenomenon is presented in reference 1, together with experimental data for a typical tapered wing showing a comparison of the true maximum lift coefficient and that defined by buffeting.

The major portion of the wind-tunnel data was obtained from tests conducted in the Ames 1- by $3\frac{1}{2}$ -foot high-speed wind tunnel and the Ames 16-foot high-speed wind tunnel, and from published reports of tests in the Langley variable-density and two-dimensional wind tunnels. Standard wind-tunnel procedures were used in all these tests.

RESULTS

The variation with Mach number of the maximum lift coefficients of the test airplanes at a constant altitude are shown in figure 4. The test altitudes varied from 20,100 feet to 32,300 feet, depending upon the airplane. The corresponding Reynolds numbers for each are presented in figure 5. For the P-39N (reference 2), P-51B, and P-63A airplanes, additional maximum-lift-coefficient data obtained at several altitudes from 5,000 to 33,000 feet are shown in figure 6 and the corresponding Reynolds number in figure 7.

It should be noted that the data for the P-39N airplane is slightly different from that originally presented in reference 2, due to correction of some small errors.

DISCUSSION

Effect of Reynolds Number on the Maximum Lift Coefficient

The variation of the maximum lift coefficient with Reynolds

number at constant Mach numbers, obtained by cross-plotting the data of figures 6 and 7, is shown in figure 8 for the P-39N, P-51B, and P-63A airplanes. The lower Mach number data of this figure show that, with increasing Reynolds numbers, the maximum lift coefficients of the P-51B and P-63A airplanes at first remain nearly constant, but increase rapidly as the Reynolds number exceeds a critical value, and finally become nearly constant again at the higher value. A similar trend is indicated by the data for the P-39N airplane although the tests were not extended to Reynolds numbers low enough to define the critical.

These effects of Reynolds number on the maximum lift coefficients are qualitatively consistent with those described in reference 3 and are explainable on the same basis. For purposes of simplification, the following generalized explanation is given. That is, the constant value of maximum lift coefficient at low Reynolds numbers is caused by laminar separation of the boundary layer; the increasing values of maximum lift coefficient beyond a critical Reynolds number occur as the boundary-layer separation changes from laminar to turbulent; and the nearly constant value of the maximum lift coefficient at the higher Reynolds numbers is produced by turbulent separation of the boundary layer. A more complete description of the mechanism of these changes is provided in reference 3. Quantitatively the Reynolds number effects found in the present tests were much smaller than those of reference 3. This difference is discussed in a subsequent section of this report.

Effects of Mach Number on the Maximum Lift Coefficient

The curves of figure 9 (obtained by cross-plotting the data of figs. 6 and 7) show that at constant Reynolds number the maximum lift coefficient of the P-39N, P-51B, and P-63A airplanes continually diminish as the Mach number increases from 0.15 to 0.40. (Application of the methods of reference 4 shows that for the measured variations of maximum lift coefficient with Mach number, the theoretically computed critical Mach numbers of the airfoils were attained at Mach numbers of approximately 0.4 for all the airplanes tested.) Figures 4 and 9 show that, as the Mach number is increased further, the maximum lift coefficients of the airplanes with conventional airfoils continue to diminish to the highest test Mach numbers; whereas those for the airplanes with low-drag airfoils reach a minimum at a Mach number between 0.40 and 0.50 and then

NACA TN No. 1044

8

begin increasing until peak values are reached at a Mach number between 0.60 and 0.66.

The decrease of the maximum lift coefficients of all the airplanes with increasing Mach number in the subcritical Mach number range may be attributed to the separation of the boundary layer at smaller angles of attack induced by the compressibility-steepened adverse pressure gradient.

The reasons for the diverse characteristics exhibited by the low-drag and conventional airfoils at supercritical Mach numbers are illustrated in figure 10 and discussed in reference 5. In brief, the pressure distributions of figure 10 indicate that as the Mach number is increased beyond the critical, a tendency for the pressure peak at the nose of the airfoil to decrease and for the low-pressure region to broaden is evidenced for both the conventional and low-drag airfoils. With the NACA 66,2-215 ($\alpha = 0.6$) low-drag airfoil, the upper-surface low-pressure region broadens considerably with increasing Mach number, more than offsetting the reduction in the pressure peak so that higher maximum lift coefficients are produced. This effect persists until at Mach numbers between 0.60 and 0.66 the loss in lift due to the decrease of the pressure peak finally offsets the addition of lift due to the broadening of the low-pressure region. With the NACA 23015 conventional airfoil, however, the negative pressure peak broadens so slightly that it is insufficient to counteract the loss in lift produced by the lowering of the pressure peak, and the maximum lift coefficient continues to decrease up to the highest Mach number of the flight tests. Meanwhile the lower-surface pressure distributions on both airfoils remain virtually unchanged throughout the Mach number range shown, indicating that the upper-surface effects account for nearly all the observed changes in maximum lift coefficient.

Interrelated Effects of Mach and Reynolds Numbers on the Maximum Lift Coefficient

While the foregoing sections have discussed the effects of Mach and Reynolds numbers on the maximum lift coefficient as though they were entirely separate and independent phenomena, the actual effects of each variable are modified to a secondary extent by the value of the other. In general, the interaction of the Mach and Reynolds number effects is such that the variation of the maximum lift coefficient with either variable remains qualitatively as described previously although modified quantitatively.

In this section, the interrelated effects of Mach and Reynolds numbers on the maximum lift coefficients of the P-39N, P-51B, and P-63A airplanes as evidenced by the curves of figures 8 and 9 are discussed. This discussion is divided into two sections corresponding, respectively, to Mach numbers less than or greater than the critical Mach number of 0.4,

Subcritical Mach number range.— The curves of figure 8 for the P-51B and P-63A airplanes show that, as the Mach number increases, the critical Reynolds number becomes greater while the characteristic effects of Reynolds number become smaller, finally disappearing at moderately supercritical Mach numbers. The same general trends may be seen in the data for the P-39N airplane although the test range does not extend to Reynolds numbers as small as the critical. Most of the interrelated effects of Mach and Reynolds numbers are best illustrated by the graphs of figure 11 and the further discussion of these phenomena will be concerned mainly with the data as plotted in that manner.

Figure 11 shows the variation with Mach number of four of the pertinent parameters describing the variation of the maximum lift coefficient with Reynolds number. These parameters are R_{cr} , the critical Reynolds number; ΔC_{Lmax} , the increment in the maximum lift coefficient as the stall changes from laminar separation to turbulent separation; $C_{Lmaxlam}$,

the maximum lift coefficient corresponding to laminar separation; and $C_{Lmaxturb}$, the maximum lift coefficient corresponding to turbulent separation. Each of these factors is illustrated by a sketch shown in figure 11. The abrupt increase in the maximum lift coefficient of the P-51B airplane shown in figure 8 at the highest Reynolds numbers at Mach numbers of 0.40 and 0.50 is essentially a supercritical Mach number phenomenon and will be discussed later,

The R_{cr} of the P-51B and P-63A airplanes are shown in figure 11(a) to vary nearly linearly with Mach number throughout the range tested. There are two effects which could cause such a variation of R_{cr} with Mach number. One is the increase of kinematic viscosity in the boundary layer of a compressible fluid due to aerodynamic heating which causes the ratio of the local Reynolds number (based on boundary-layer conditions) to the free-stream Reynolds number to diminish as shown in reference 6. Accordingly, as shown by references 7 and 8, a larger free-stream Reynolds number would be necessary to reach the local critical Reynolds

numbers required for transition from a laminar to a turbulent boundary layer. A second possibility is due to the fact that increasing the Mach number in the subcritical range has effects on the upper-surface pressure distributions similar to that of decreasing the airfoil thickness. The pressure peaks become sharper and the adverse pressure gradients become steeper. Decreasing the airfoil thickness is shown in reference 3 to increase R_{cr} , hence similar effects due to increasing Mach number would be anticipated.

Figure 11(b), which shows the variation with Mach number of $\Delta C_{L_{max}}$ for the P-51B and P-63A airplanes, indicates that $\Delta C_{L_{max}}$ decreases with increasing Mach number, finally becoming zero at Mach numbers between 0.50 and 0.60. To afford a better understanding of this effect curves of $C_{L_{max_{lam}}}$ and $C_{L_{max_{turb}}}$ are plotted as a function of Mach numbers in figure 11(c). These curves show that, while both parameters decrease as the Mach number is increased, $C_{L_{max_{turb}}}$ decreases at a much greater rate than $C_{L_{max_{lam}}}$.

This characteristic probably may be attributed partially to the higher local Mach numbers involved at the larger lift coefficient of $C_{L_{max_{turb}}}$ causing the adverse pressure gradients to be steepened more than those corresponding to $C_{L_{max_{lam}}}$. Another contributing factor may be that the turbulent separation, originating at the trailing edge, is affected by the compressibility-steepened adverse pressure gradient along the entire chord, while the laminar separation, occurring near the leading edge, would be influenced mainly by the steepened pressure gradients over only a small portion of the chord.

Supercritical Mach number range.— At supercritical Mach numbers, figures 8 and 9 show that the maximum lift coefficient continues to vary rapidly with changes of Mach number and that the usual Reynolds number effects, as described previously, become negligibly small at Mach numbers of 0.55 for all the airplanes tested.

With the P-51B airplane, however, an unusual effect of Reynolds number was indicated which may have significance as a general type of phenomenon possible at supercritical Mach numbers. Figure 8 shows that at moderately supercritical Mach numbers and at Reynolds numbers greater than those at which the previously discussed variation of maximum lift

coefficient with Reynolds number occurs, the maximum lift coefficient increased abruptly as the Reynolds number was increased. The entire effect disappeared at Mach numbers greater than about 0.60. The curves of figure 6 for the F-51B airplane show that the Mach number at which the maximum lift coefficient starts to increase when in the supercritical Mach number range is nearly constant at a value of 0.49 for all altitudes tested above 17,300 feet, corresponding to Reynolds numbers less than 13,700,000. At lower test altitudes, or larger Reynolds numbers, however, the maximum lift coefficient reaches its minimum value at a lower Mach number. Since increasing values of the maximum lift coefficient with increasing Mach numbers in the supercritical Mach number region have been shown to be caused by the rearward movement of the shock wave, it appears that these Reynolds number effects at supercritical Mach numbers are more the result of the boundary layer influencing the shock-wave position than the result of the normal boundary-layer separation, whether laminar or turbulent, being modified by compressibility effects as at subcritical Mach numbers. Further research is necessary before a complete understanding of this phenomenon is had.

Comparison of Flight and Wind-Tunnel Data

In order to determine whether the general effects of Mach and Reynolds numbers indicated by the flight data are adequate to permit correlation of flight and wind-tunnel results, wind-tunnel data, although obtained at combinations of Mach and Reynolds numbers not covered in flight, are compared with the flight data. In successive divisions of this section, the flight data will be compared with wind-tunnel data obtained for models tested in the Ames and Langley 16-foot high-speed wind tunnels, those obtained for several airfoils in the Ames 1- by $3\frac{1}{2}$ -foot high-speed wind tunnel, and those obtained for several airfoils in the Langley variable-density and two-dimensional wind tunnels.

Comparison of flight data with model data from Ames and Langley 16-foot high-speed wind tunnels.— Maximum lift-coefficient data obtained on models of the P-38, P-39N, and XP-80 airplanes in the Ames 16-foot high-speed wind tunnel and corrected for trim are presented in figure 12, together with the high-altitude flight data of figure 4 for the corresponding airplanes. The Reynolds numbers for the tunnel tests are shown in figure 5 to be considerably lower than those of the flight tests. A comparison of the maximum lift coefficients

obtained from flight and wind-tunnel data indicates that, although the same qualitative effects of Mach number are shown in all the data, absolute agreement between the actual values of the coefficients measured in flight and in the tunnel does not always exist. Most of the discrepancies, however, may be accounted for by a consideration of all the pertinent variables. In general, considering only the difference between the Reynolds numbers of the flight and wind-tunnel tests, the comparison should show close agreement existing at the higher Mach numbers but lower maximum lift coefficients for the tunnel data than for the flight data at the lower Mach numbers. Actually the data for the various airplanes show deviations from this trend which are of magnitudes that can be related directly to the relative aerodynamic cleanliness of the designs as discussed in reference 9. Thus the maximum lift coefficients of the YP-80A airplane, which had smooth wing surfaces and no propeller, showed excellent agreement with the expected trends; those of the P-39N airplane, which had a rougher surface finish, considerable air leakage, and an idling propeller, were somewhat lower than the wind-tunnel values. Although the maximum lift coefficients of the P-38F airplane were affected by the items mentioned for the P-39N, perhaps an even more important factor for this airplane was the distortion of the lift curves at high Mach numbers by compressibility effects.

The importance of this latter consideration is indicated by the curves of figure 13 which show the variation of the lift coefficient with angle of attack for models of the P-39N, XP-80, and P-38 airplanes as measured at several Mach numbers in the Ames 16-foot high-speed wind tunnel. In contrast to the lift curves of the P-39N and XP-80 models, which are nearly straight lines until near the maximum lift coefficient, those of the P-38 model have a definite decrease in slope at moderate angles of attack known, in this case, to result from air-flow separation over the wing center section. The actual maximum lift coefficient of the P-38 model then occurs at extremely high angles of attack. Similar effects were measured at supercritical Mach numbers in tests of a tapered wing of NACA 230-series airfoil sections conducted in the Langley 16-foot high-speed wind tunnel and reported in reference 1. At Mach numbers above 0.55 the angle of attack at which the maximum lift coefficient was reached was 10° to 12° higher than that at which pronounced separation of the flow occurred. Consequently, the concept of a range of maximum obtainable lift coefficients at high Mach numbers was introduced. This range extends from the lift coefficient corresponding to the initial stall (arbitrarily defined as being at 2° to 3° above the

angle of attack at which separation of the flow from the wing initially occurs) to that corresponding to the actual maximum lift coefficient of the wing. As the initial stall lift coefficient is exceeded, increases in stability and tail buffeting are likely to occur. These may become sufficiently great that they would appear to the pilot to define the maximum lift coefficient obtainable in flight.

Accordingly, initial-stall and maximum-lift-coefficient points for the P-38 model, as obtained from figure 13, are plotted in figure 12. It may be seen that good agreement exists between the flight maximum lift coefficient and the initial-stall lift coefficient of the model. Similarly, flight data for the F6F-3 airplane, the wing of which is similar to the wing model, agree with the wing model data corresponding to the initial stall rather than to the maximum lift coefficient. (The Reynolds number of the tapered wing tests is shown in fig. 5.) Such considerations have little effect on the P-39N and XP-80 model data, however, since the initial-stall lift coefficient is virtually equal to the maximum lift coefficients for both models. It appears, therefore, that the maximum lift coefficient obtainable in flight may be better estimated by considering the value of the initial-stall lift coefficient of a model rather than its actual maximum lift coefficient.

Comparison of flight data with Ames 1- by 3 $\frac{1}{2}$ -foot high-speed airfoil data.—Maximum-lift-coefficient data obtained in the Ames 1- by 3 $\frac{1}{2}$ -foot high-speed wind tunnel for two-dimensional models of the NACA 23015, 0015, 66.2-215 and 66 $\frac{1}{2}$ -212 airfoils which are approximately similar, respectively, to the root sections of the P-38F and F6F-3, P-39N, P-51B and P-63A, and YP-80A airplanes, are presented in figure 14, together with the high-altitude flight data from figure 4 for these airplanes. For the airfoils and Mach number ranges of figure 14, no appreciable difference existed between the initial-stall lift coefficient and the maximum lift coefficient. The Reynolds numbers of the tunnel tests are shown in figure 5.

Because of the many differences between a two-dimensional airfoil model in a wind tunnel and an airplane in flight, only qualitative verification of the trends indicated by the flight data should be anticipated and any close quantitative agreement is probably merely coincidental. At the higher Mach numbers, very similar effects of Mach number are experienced by the airplanes and the airfoils; in fact, close quantitative

agreement exists in every case except between that of the F-38F airplane and the NACA 23015 airfoil. At lower Mach numbers, however, the maximum lift coefficients of the airfoils have lower values, and are less affected by changes of Mach number than those of the airplanes with which they are compared. These trends are in accord with the previously discussed effects of Reynolds number which are large at low Mach numbers and decrease in magnitude as the Mach number becomes greater.

Comparison of flight data with Langley variable-density-tunnel and two-dimensional-tunnel airfoil data.— Figures 15(a) and 15(b) show the variation with effective Reynolds number of the maximum lift coefficient of several NACA conventional airfoils as measured in the Langley variable-density wind tunnel (reference 3). These airfoils were three-dimensional models having an aspect ratio of 6. Since the tunnel was operated at constant speed and the Reynolds number was changed by varying the pressure, the Mach number was almost exactly constant at a value of 0.06 throughout the entire Reynolds number range. The data are presented in two groups, figure 15(a) showing the effects of changes of thickness ratio and figure 15(b) showing the effects of changes of camber. These curves show that $CL_{max_{lam}}$ is a very sensitive function of camber but relatively independent of thickness, while R_{cr} varies greatly with thickness but only slightly with camber. Both camber and thickness affect $CL_{max_{turb}}$ however, but to a much lesser extent than they do $CL_{max_{lam}}$ or R_{cr} . Values of the maximum lift coefficients of several two-dimensional NACA low-drag airfoil models tested in the Langley two-dimensional wind tunnel at three Reynolds numbers (approximately 3,000,000, 6,000,000, and 9,000,000) are presented in figure 15(c). The various Reynolds numbers were obtained by simultaneous changes of pressure and airspeed, the Mach numbers corresponding to the listed test Reynolds numbers being approximately 0.10, 0.14, and 0.15, respectively. Due to the limited Reynolds number range of these latter tests, the value of R_{cr} , $CL_{max_{lam}}$, and ΔCL_{max} are unknown, and of the four parameters only $CL_{max_{turb}}$ is determinable.

A comparison of these airfoil data with the flight data of figure 8 shows that the variation of the maximum lift coefficient with Reynolds number was much less for the flight tests than for the tunnel tests and that the R_{cr} was much higher for the flight tests. These apparent discrepancies,

however, may be accounted for by a consideration of the effects resulting from the difference between the Mach number of the flight and tunnel tests. Since wind-tunnel data of the nature of figure 15 were not available for the exact airfoils used on the test airplanes, airfoils used for comparison with the flight results were selected in accordance with the previously discussed relations shown in figures 15(a) and 15(b). Thus, the airplane CL_{maxlam} and ΔCL_{max} data are compared in figure 11 only with those of airfoils having about the same amount of camber as the airfoils used on the airplanes; whereas the airplane $CL_{maxturb}$ data, being relatively insensitive to changes of thickness and camber, are compared with similar data for all the airfoils of figure 15.

Since the Reynolds numbers of the tunnel tests did not quite extend to the point of $CL_{maxturb}$ for some of the NACA conventional airfoils, the data were extrapolated slightly and the resulting values plotted in figure 11. In each of the comparisons in figures 11(b) and 11(c) it may be seen that, although the variation of the maximum lift coefficient with Reynolds number was much less for the flight tests than for the tunnel tests, the apparent discrepancies between the Reynolds number effects observed in flight and in the Langley variable-density and two-dimensional wind tunnels may be accounted for by extrapolating the trends indicated by the flight data to very low Mach numbers.

Values of R_{cr} of the airfoils are not shown for comparison with the flight data for the following reason. The flight data were obtained only for the P-51B and P-63A airplanes, which have NACA low-drag airfoils; whereas the only wind-tunnel R_{cr} values available were for NACA conventional airfoils. Values of R_{cr} for NACA conventional airfoils were not believed to be suitable for comparison with those for NACA low-drag airfoils since R_{cr} has been shown to be a very sensitive function of thickness ratio and would, therefore, probably vary considerably with changes of thickness distribution, particularly near the leading edge. It is significant to note, however, that for each of the NACA low-drag airfoils for which data are shown in figure 15(c), R_{cr} has been exceeded at the lowest test Reynolds number of 3,000,000 and Mach number of 0.10. Such low values of R_{cr} are consistent with the trends indicated by the flight data.

Correlation of Maximum-Lift-Coefficient Data from Several Wind Tunnels

In early efforts to correlate low-speed airfoil data obtained in various wind tunnels having different degrees of turbulence, the concept of a "turbulence factor" was introduced in references 10 and 11 as a multiplier of the test Reynolds number to obtain an effective Reynolds number equivalent to nonturbulent free-air conditions. This factor alone did not prove sufficient for correlating maximum-lift-coefficient data. The data of this report, however, suggests the possibility that similar data obtained on airfoil models tested in various wind tunnels may be correlated by a consideration of the effects of Mach number, as well as Reynolds number.

Accordingly, from maximum-lift-coefficient data measured in six wind tunnels on models of the NACA 0012 and 0012-63 airfoils, which are very similar, values corresponding to several effective Reynolds numbers were selected from faired curves in the reference reports and replotted in figure 16 as a function of Mach number. The test conditions are summarized in table I.

The data from these wind tunnels indicate that it may be possible to correlate the maximum lift coefficients obtainable in various wind tunnels by considering the Mach number as well as the turbulence factor, even though the Mach number may be very small. These curves for the NACA 0012 airfoil are very similar to those previously observed in the flight data. It is shown that the maximum lift coefficient is affected by Mach numbers as low as 0.15 and that the Reynolds number effects decrease with increasing Mach number, as indicated by the flight test data. Similar plots of maximum lift data have been made for several other airfoils. Although the quantity of data for any of the other airfoils is not so great as that for the NACA 0012 airfoil, trends similar to those shown in figure 16 are readily apparent for all the airfoils.

CONCLUSIONS

An analysis of the effects of Mach and Reynolds numbers on the maximum lift coefficients of several airplanes and wind-tunnel models has resulted in the following conclusions:

1. When the effects of Mach number were considered, as well as those of Reynolds number, good correlation was found between flight data and available wind-tunnel data, provided buffeting or other factors did not prevent attainment of the actual maximum lift coefficient in flight, in which case the maximum lift coefficient obtained in flight appeared to be related to a pronounced decrease in lift-curve slope. The same considerations provided good agreement among limited airfoil data from various wind tunnels. Data indicated that the maximum lift coefficient was affected by Mach number down to Mach numbers of approximately 0.15.

2. Distinct differences exist between the effects of Mach and Reynolds numbers on the maximum lift coefficient in the subcritical and supercritical Mach number regions.

3. In the subcritical Mach number region, the maximum lift coefficient obtainable in flight by the airplanes tested decreased steadily with increasing Mach number. As the Mach number was increased in the supercritical Mach number region, the maximum lift coefficient of NACA conventional airfoils continued to diminish as at subcritical Mach numbers, while that of NACA low-drag airfoils reached a minimum at a Mach number between 0.40 and 0.55 and then began increasing until secondary peak values were reached at a Mach number between 0.60 and 0.66.

4. In the subcritical Mach number region, effects of Reynolds number on the maximum lift coefficient were qualitatively as described in NACA Report No. 586; quantitatively, the effects of Reynolds number on the maximum lift coefficient decreased progressively with increasing Mach number, becoming nil at a Mach number of approximately 0.55. The critical Reynolds number increased nearly linearly with Mach number.

5. At supercritical Mach numbers, no effects of Reynolds number were apparent for two of the three airplanes on which pertinent data were obtained; on the third airplane the maximum lift coefficient was affected by Reynolds number but in a manner basically different from that experienced at subcritical Mach numbers.

Ames Aeronautical Laboratory,
National Advisory Committee for Aeronautics,
Moffett Field, California, March 28, 1946.

REFERENCES

1. Pearson, E. O., Jr., Evans, A. J., and West, F. E., Jr.; Effects of Compressibility on the Maximum Lift Characteristics and Spanwise Load Distribution of a 12-Foot-Span Fighter-Type Wing of NACA 230-Series Airfoil Sections, NACA ACR No. 15G10, 1945.
2. Nissen, James M., and Gadeberg, Burnett L.: Effect of Mach and Reynolds Numbers on the Power-Off Maximum Lift Coefficient Obtainable on a P-39N-1 Airplane as Determined in Flight, NACA ACR No. 4F28, 1944.
3. Jacobs, Eastman N., and Sherman, Albert: Airfoil Section Characteristics as Affected by Variations of the Reynolds Number. NACA Rep. No. 586, 1937.
4. Heaslet, Max. A.; Critical Mach Numbers of Various Airfoil Sections. NACA ACR No. 4G18, 1944.
5. Stack, John, Fedziuk, Henry A., and Cleary, Harold E.: Preliminary Investigation of the Effect of Compressibility on the Maximum Lift Coefficient. NACA ACR, Feb. 1943.
6. Allen, H. Julian, and Nitzberg, Gerald E.: The Effect of Compressibility on the Growth of the Laminar Boundary Layer on Low-Drag Wings and Bodies, NACA ACR, Jan. 1943.
7. von Kármán, Th., and Millikan, C. B.: A Theoretical Investigation of the Maximum-Lift Coefficient. Jour. Appl. Mechanics, vol II, no. 1, March 1935, pp. A-21, A-27.
8. Goldstein, S.: Modern Developments in Fluid Dynamics, Vol. II, Oxford Univ. Press, 1938, pp. 478, 489.
9. Sweberg, Harold H., and Dingeldein, Richard C.: Summary of Measurements in Langley Full-Scale Tunnel of Maximum Lift Coefficients and Stalling Characteristics of Airplanes, NACA ACR No. 15C24, 1945.
10. Jacobs, Eastman N., and Clay, William C.: Characteristics of the N.A.C.A. 23012 Airfoil from Tests in the Full-Scale and Variable-Density Tunnels. NACA Rep. No. 530, 1935.

11. Platt, Robert C.: Turbulence Factors of N.A.C.A. Wind Tunnels as Determined by Sphere Tests. NACA Rep, No. 558, 1936.
12. Goett, Harry J., and Bullivant, W. Kenneth: Tests of N.A.C.A. 0009, 0012, and 0018 Airfoils in the Full-Scale Tunnel. NACA Rep. No. 647, 1938.
13. Muse, Thomas C.: Some Effects of Reynolds and Mach Numbers on the Lift of an NACA 0012 Rectangular Wing in the NACA 19-Foot Pressure Tunnel. NACA CB No. 3E29, 1943.
14. Hilton, W. F., Cowdrey, C. F., and Hyde, G. A. M.: Tests of NACA 0012-63 Aerofoil in the High Speed Tunnel. A.R.C. 4715, Sept, 1940.
15. Doetsch, H., and Kramer, M.: Systematic Airfoil Tests in the Large Wind Tunnel of the DVL. NACA TM No. 852, 1938.
16. Richter, G.: Messungen am Profil NACA 0012-63 im DVL - Hochgeschwindigkeits-Windkanal. Report No. 127 Lilienthal-Gesellschaft für Luftfahrtforschung, Sept. 1940.

TABLE I

SUMMARY OF TEST CONDITIONS FOR NACA 0012 AND 0012-63 AIRFOILS AS CONDUCTED IN SEVERAL WIND TUNNELS

Item	Langley full- scale tunnel	Langley variable- density tunnel	Langley 19-foot pressure tunnel	NPL 1-foot high-speed tunnel	DVL 5- by 7- meter tunnel	DVL 2.7-meter high-speed tunnel
Turbulence factor	1	2.64	1	1	1.1	1
Airfoil	NACA 0012	NACA 0012	NACA 0012	NACA 0012-63	NACA 0012	NACA 0012-63
Aspect ratio	6	6	6	Infinite	5	2.7 ¹ with end plates
Chord (in.)	72	5	24	2	31.50	19.69
Minimum effective Reynolds number	1,800,000	450,000	1,100,000	440,000	1,200,000	5,900,000
Maximum effective Reynolds number	4,500,000	8,400,000	8,200,000	570,000	3,500,000	(¹)
Minimum Mach number	0.04	0.06	0.06	0.40	0.06	0.68
Maximum Mach number	0.11	0.06	0.38	0.55	0.17	(¹)
Reference	12	3	13	14	15	16

¹Only one test point obtained.

NACA TN No. 1044

NACA TN No. 1044

Fig. 1

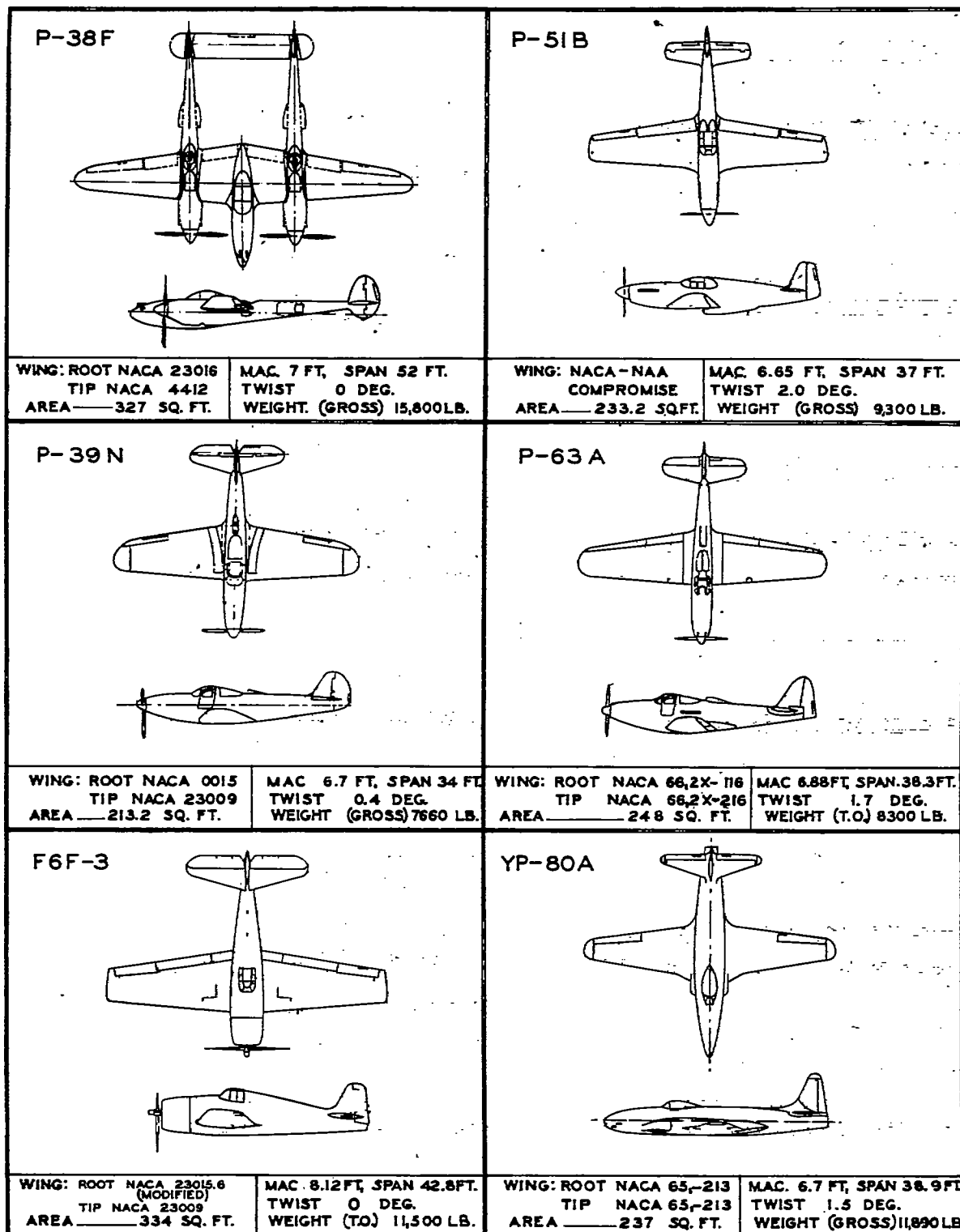
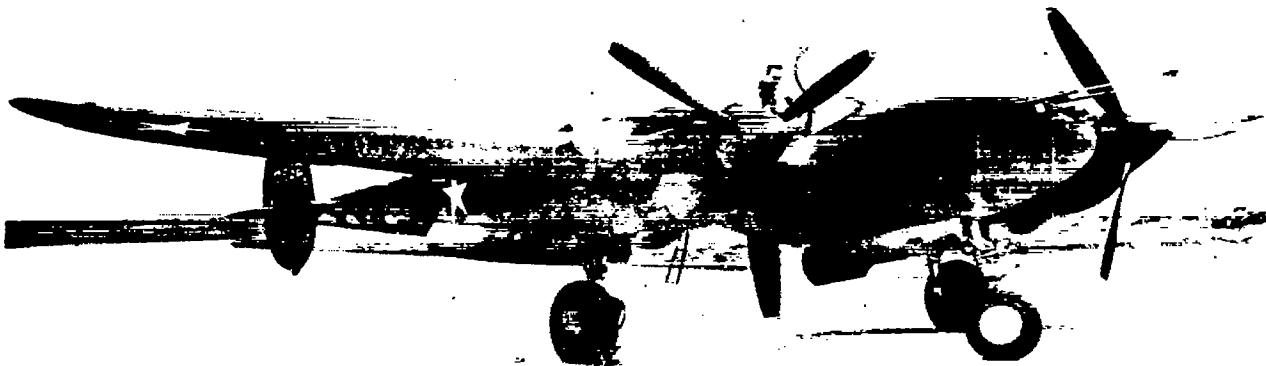
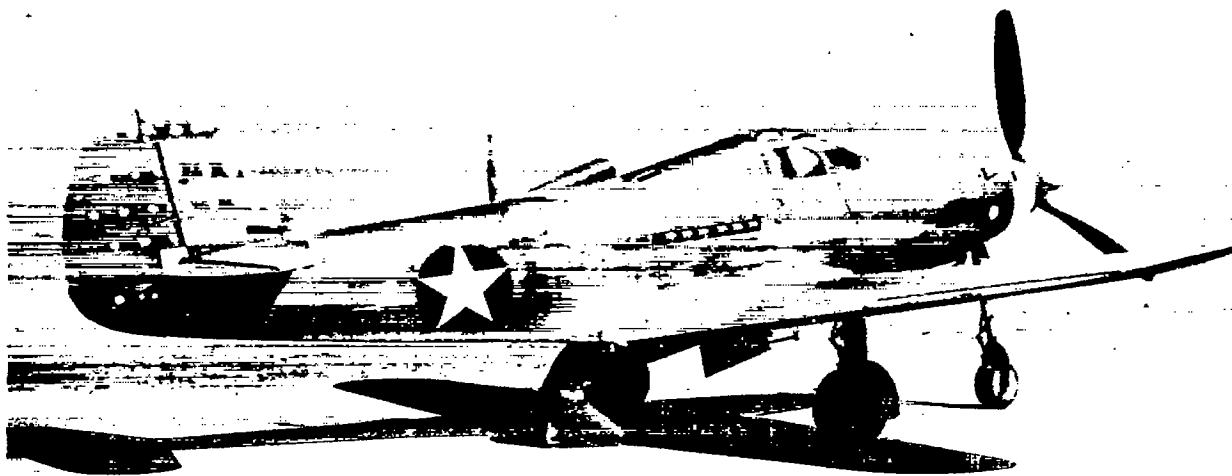


FIGURE 1.— TWO-VIEW DRAWINGS AND PERTINENT SPECIFICATIONS
 OF THE AIRPLANES TESTED IN FLIGHT.

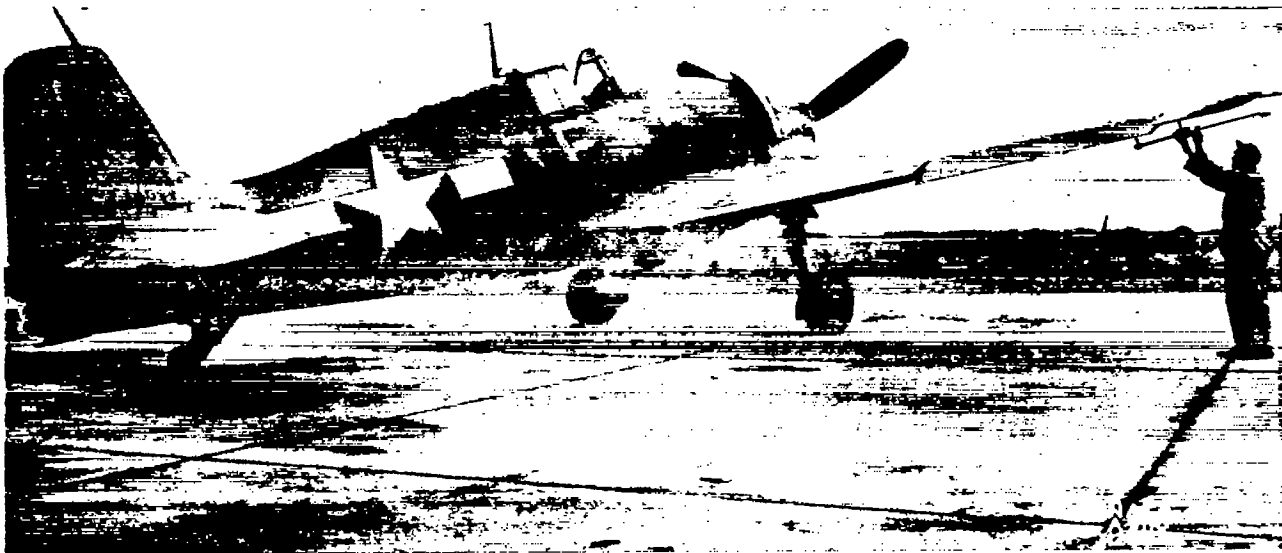


(a) P-38F airplane.

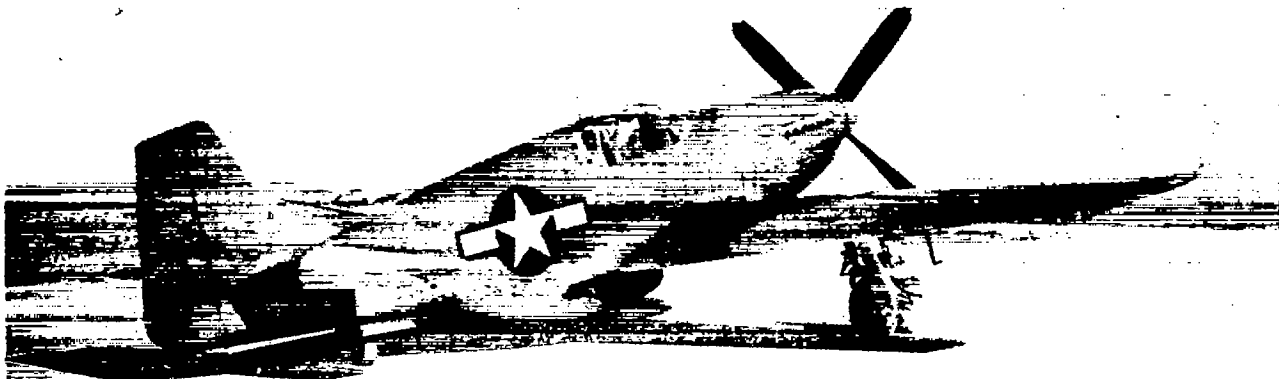


(b) P-39N airplane.

Figure 2(a to i).- Photographs of test airplanes and wind-tunnel models.



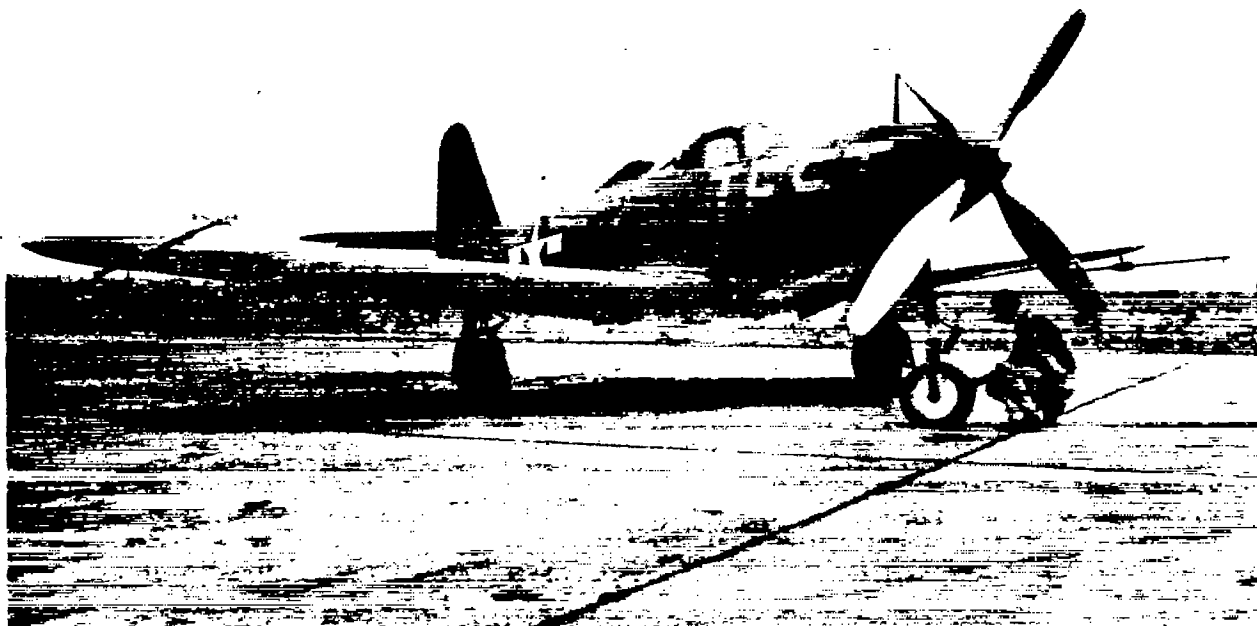
(c) F6F-3 airplane.



(d) P-51B airplane.

NACA TN No. 1044

Fig. 2e,f

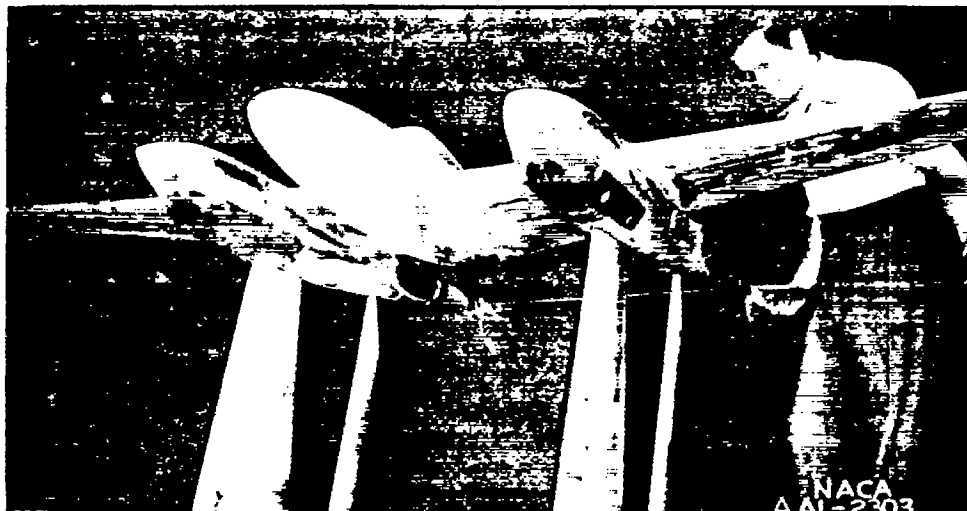


(e) P-63A airplane.

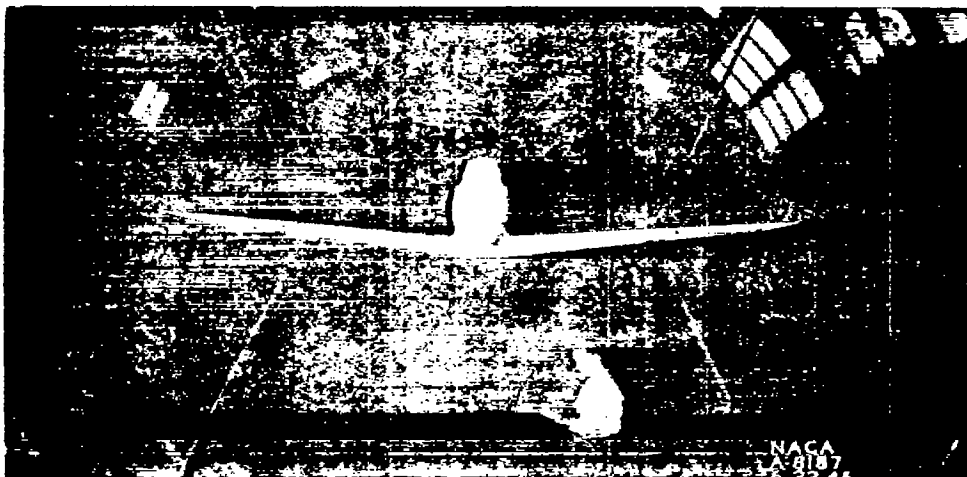


(f) YP-80A airplane.

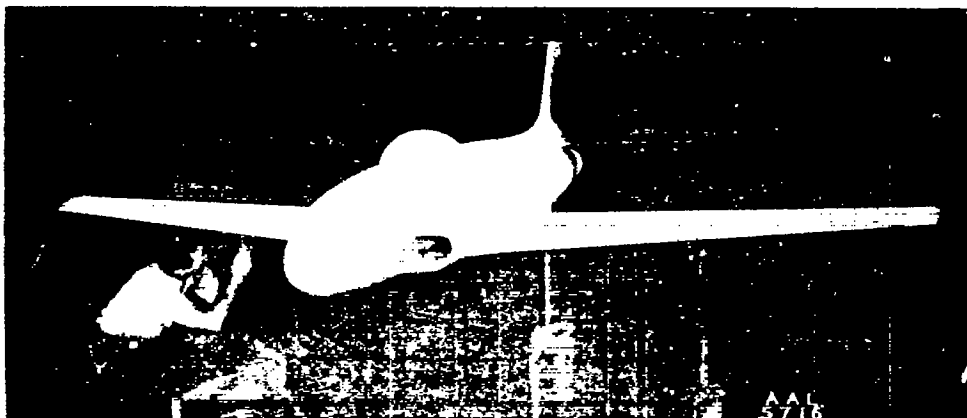
Figure 2.- Continued.



(g) Model of P-38 in Ames 16-foot high-speed wind tunnel.



(h) Model of P-39N in Ames 16-foot high-speed wind tunnel.



(i) Model of XP-80 airplane in 16-foot high-speed wind tunnel.

NACA TN No. 1044

Fig. 3

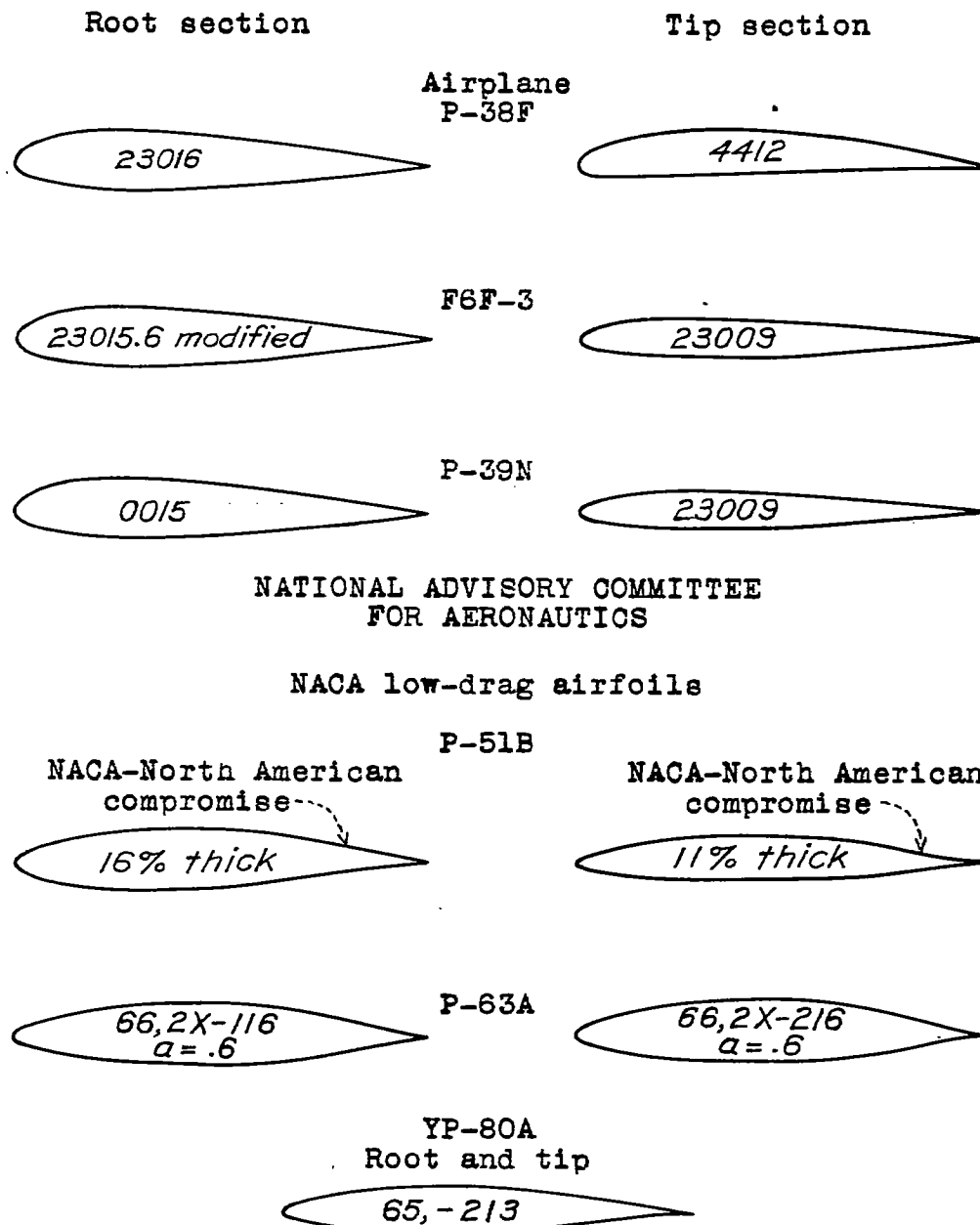


Figure 3.- Profiles of the wing root and tip sections of the test airplanes.

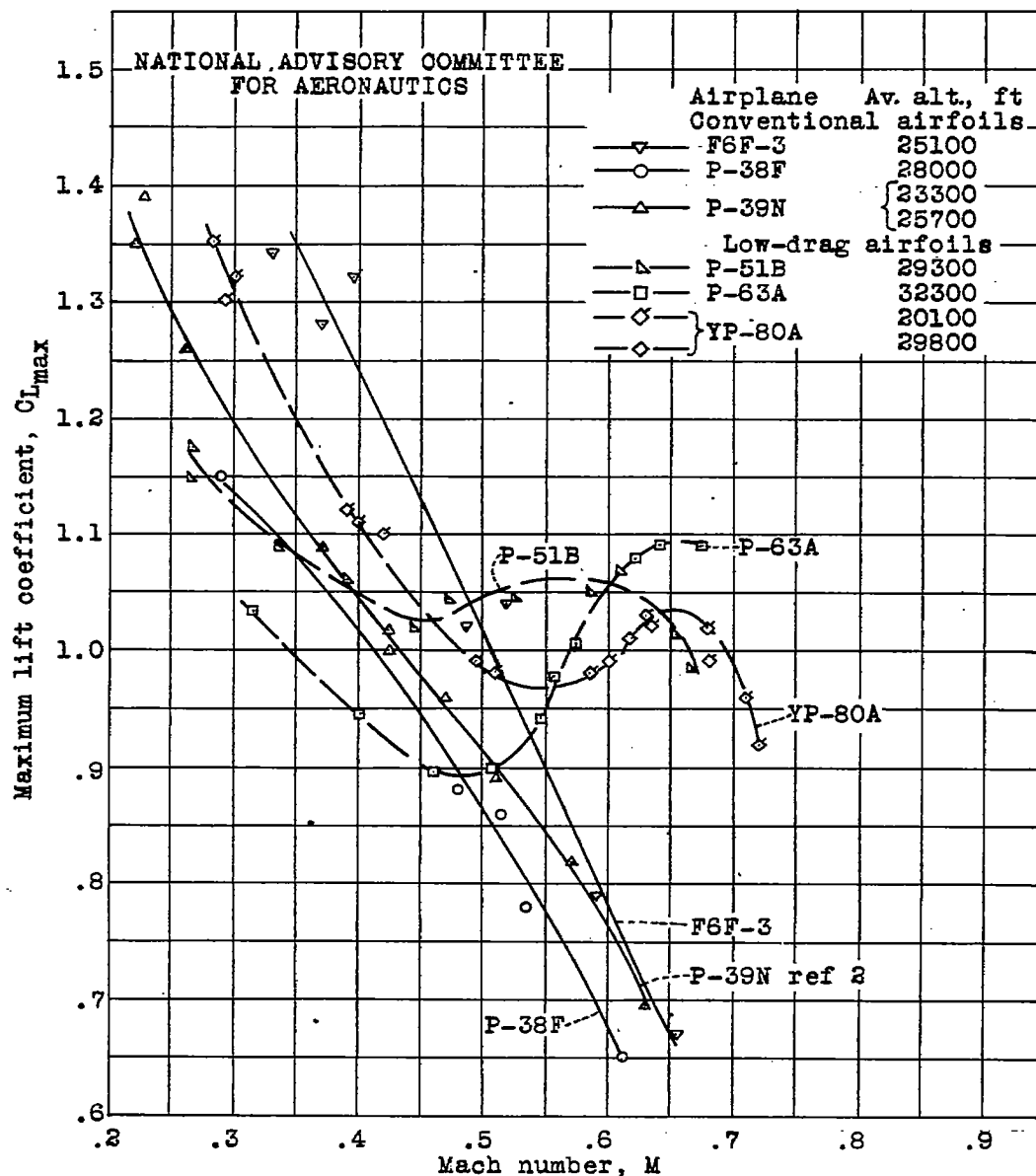


Figure 4.- Variation of maximum lift coefficient with Mach number at high altitude.

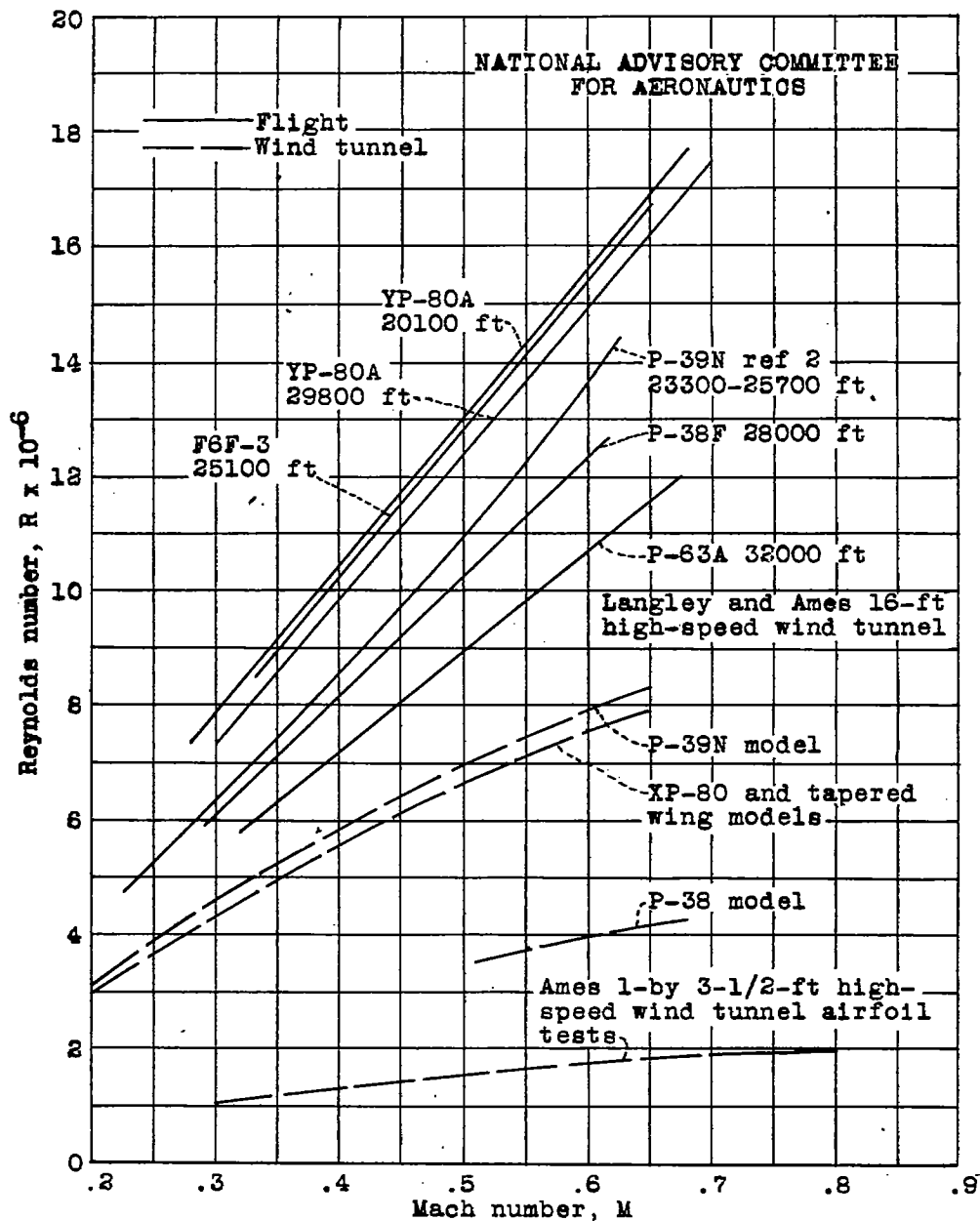


Figure 5.- Variation of Reynolds number with Mach number for the flight test data of figure 4 and the tests in the Langley and Ames 16-foot high-speed wind tunnels and the Ames 1-by 3-1/2-foot high-speed wind tunnel.

NACA TN No. 1044

Fig. 6

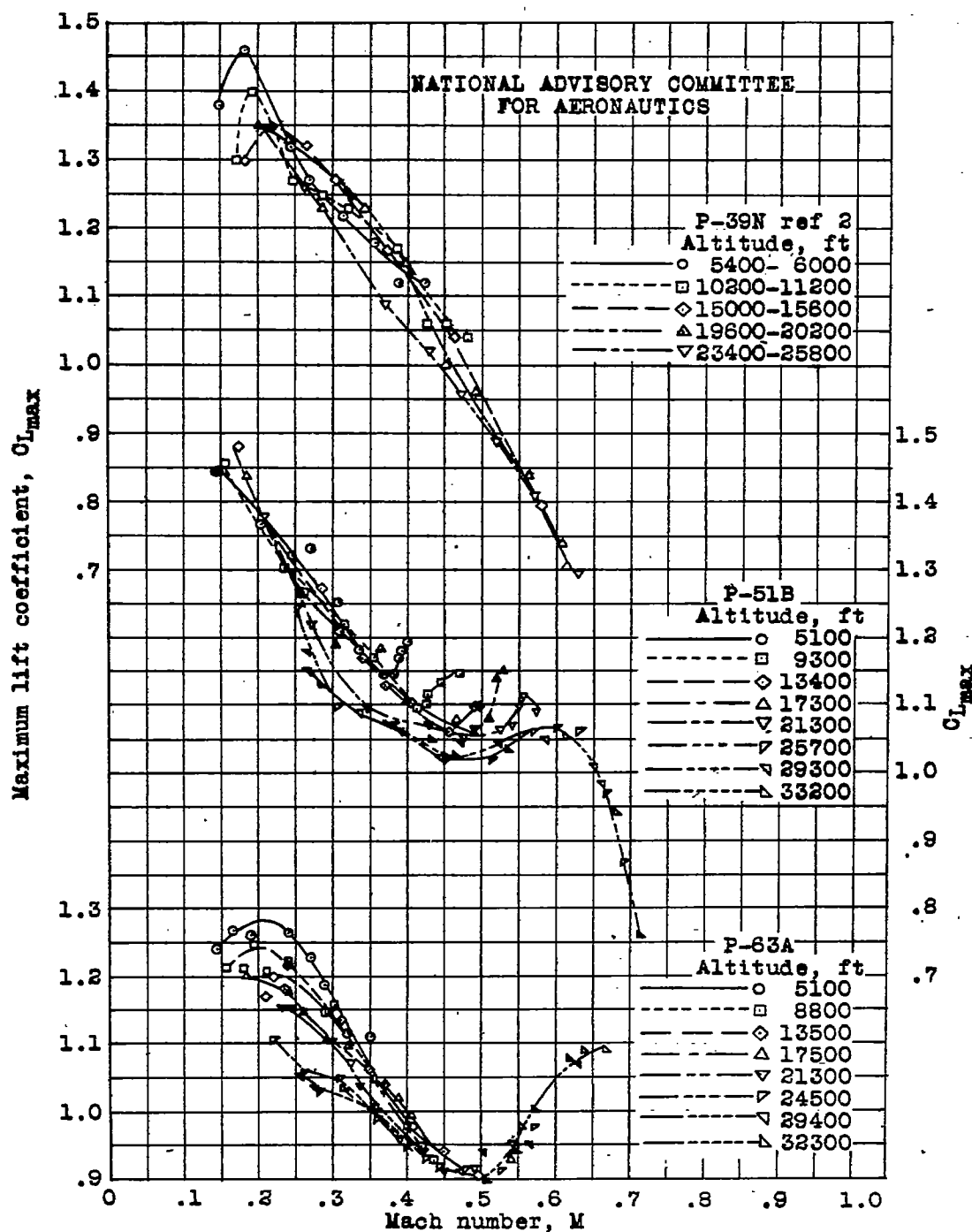


Figure 6.— Variation of maximum lift coefficient with Mach number for various altitudes.

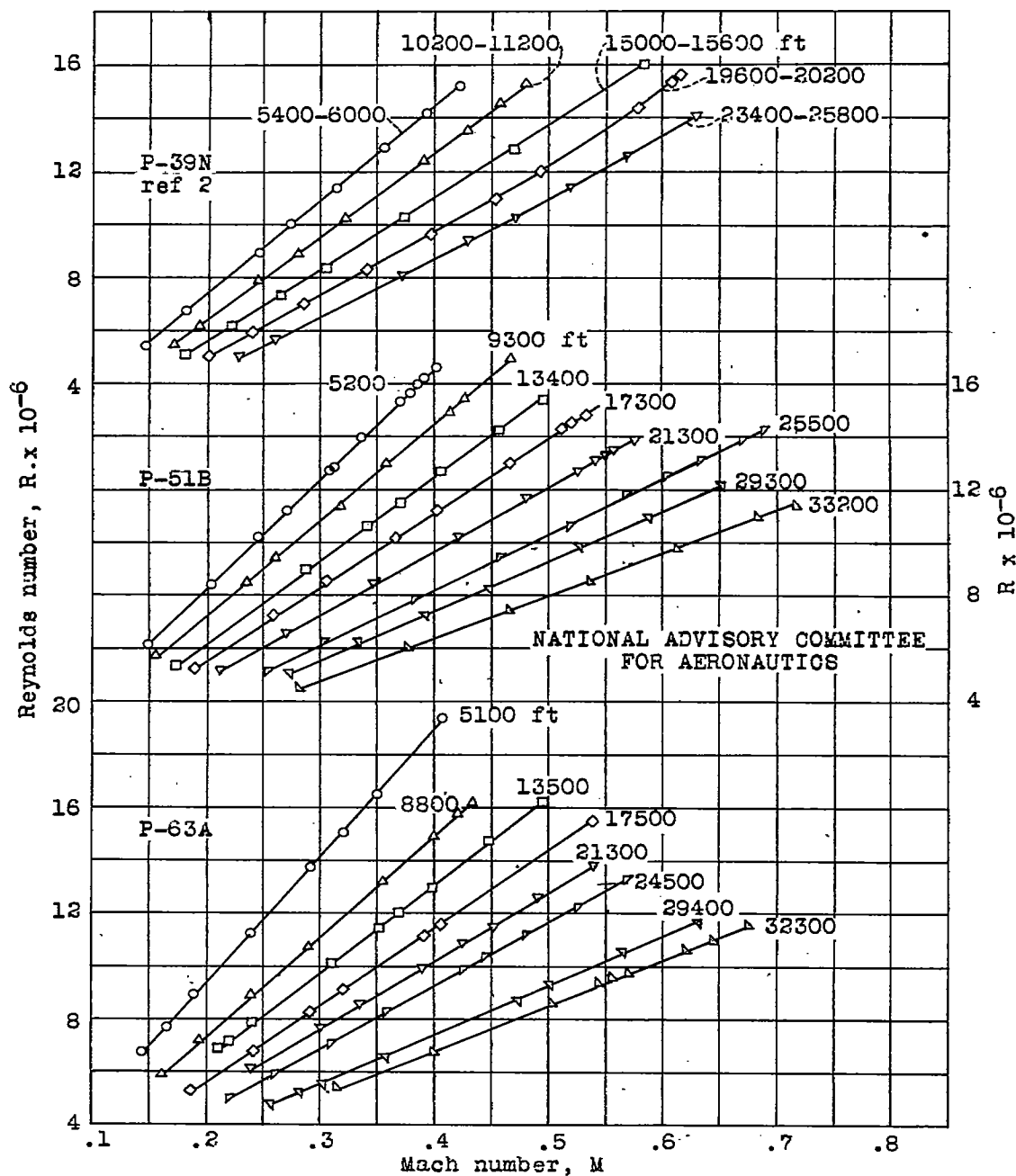


Figure 7.- Variation of Reynolds number with Mach number for the flight test data of figure 6.

NACA TN No. 1044

Fig. 8

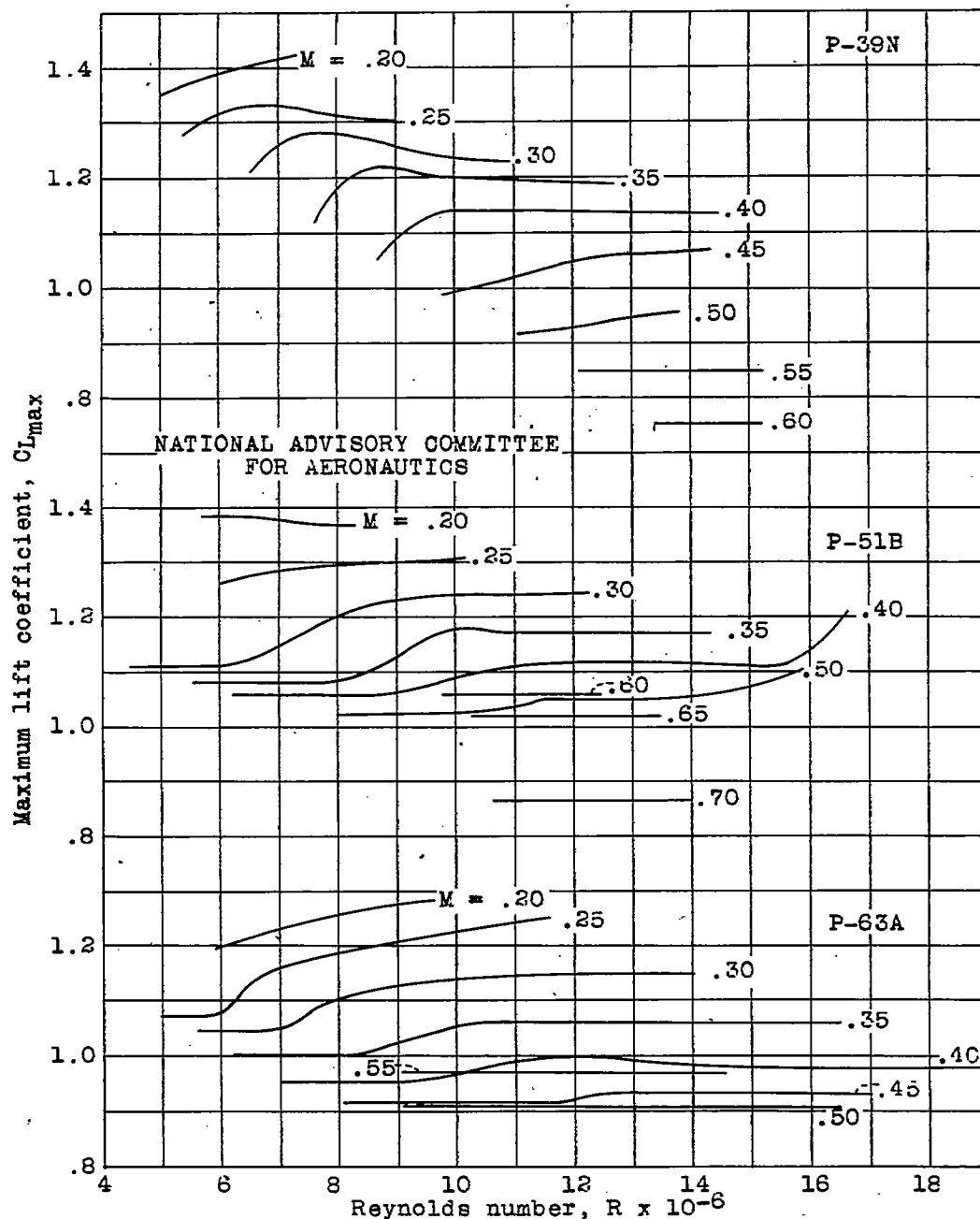


Figure 8.- Variation of maximum lift coefficient with Reynolds number for constant Mach numbers.

NACA TN No. 1044

Fig. 9

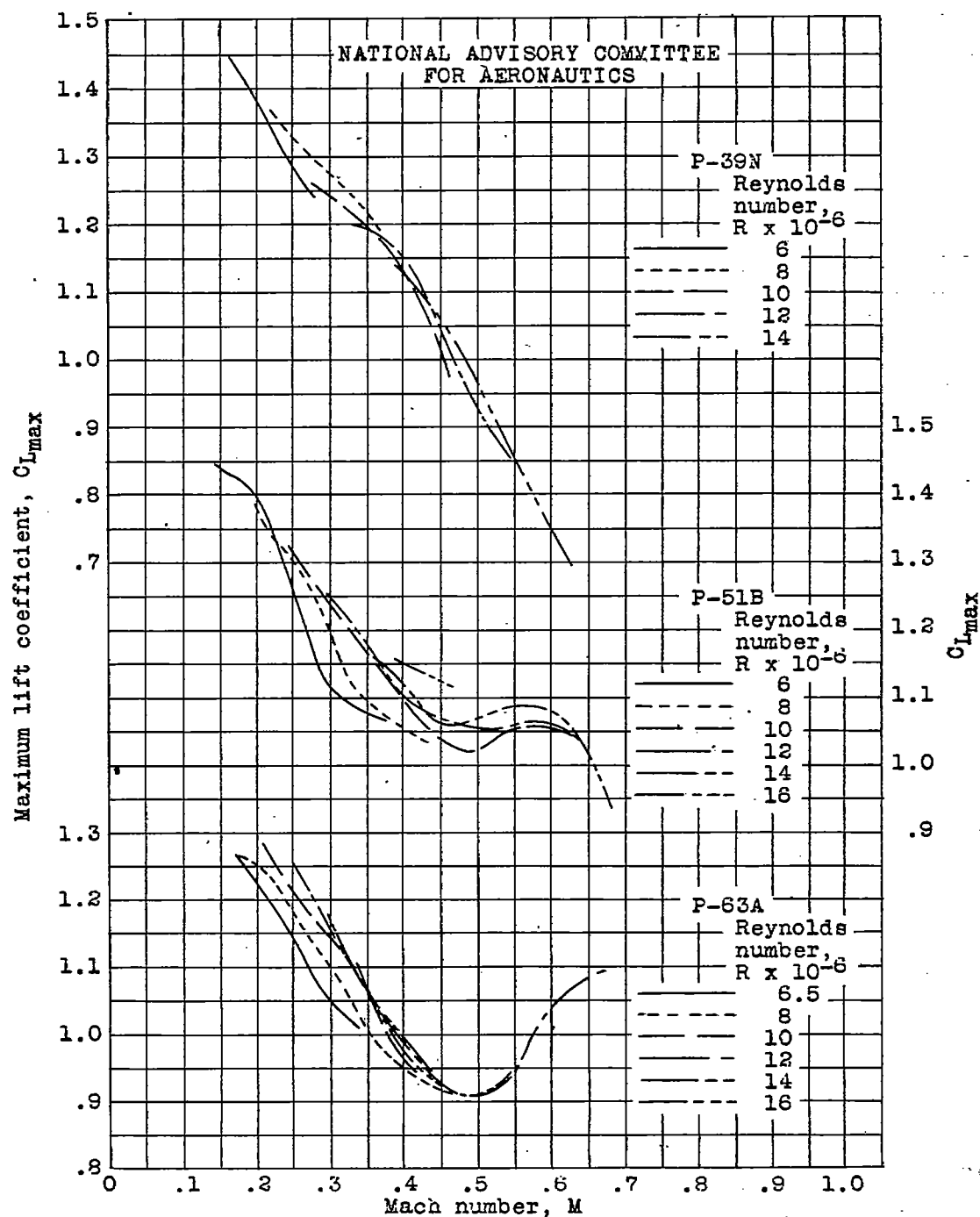


Figure 9.- Variation of maximum lift coefficient with Mach number for various Reynolds numbers.

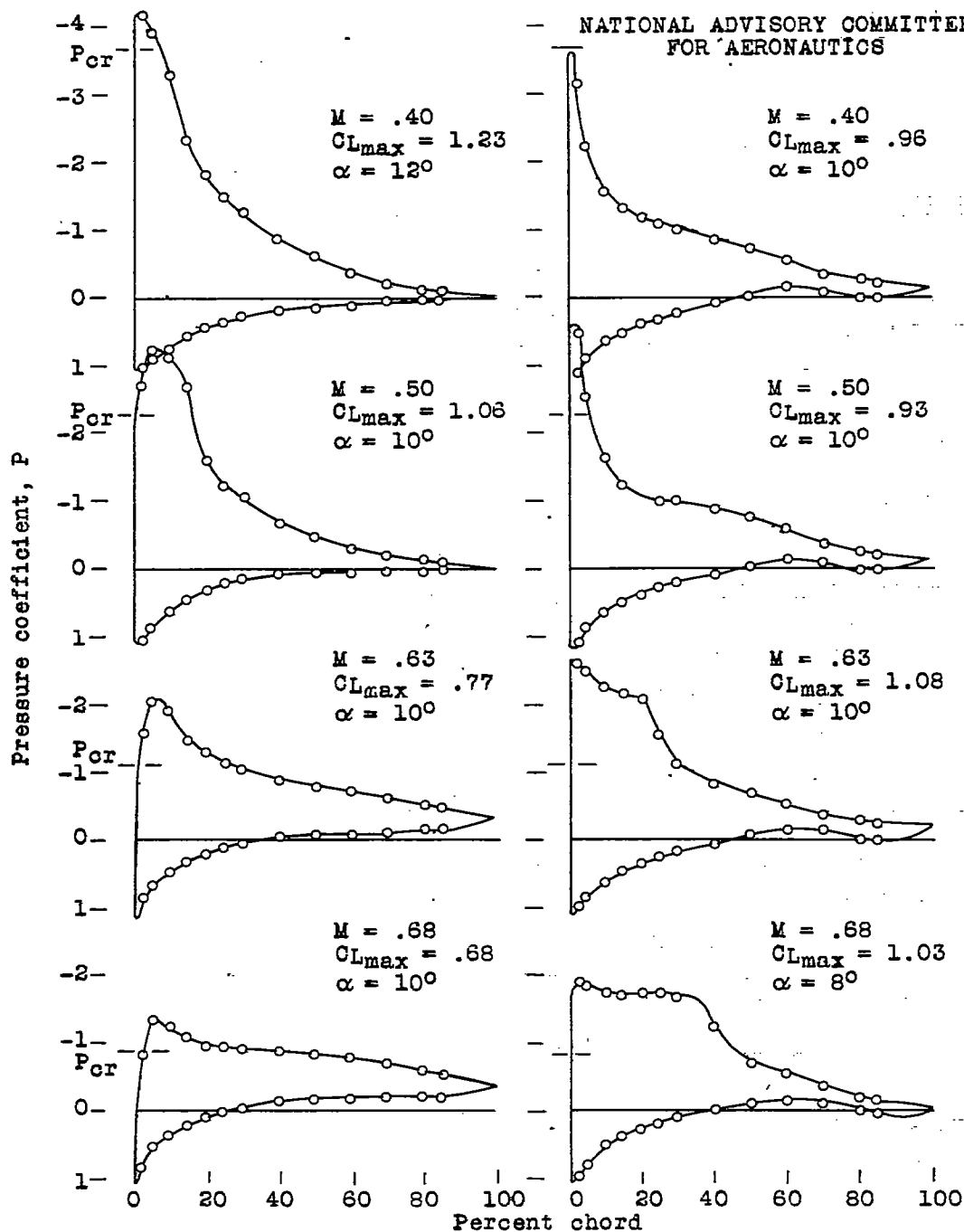


Figure 10.- Typical pressure distributions on NACA conventional and low-drag airfoils at maximum lift coefficient. Ames 1-by 3-1/2-foot high-speed wind tunnel.

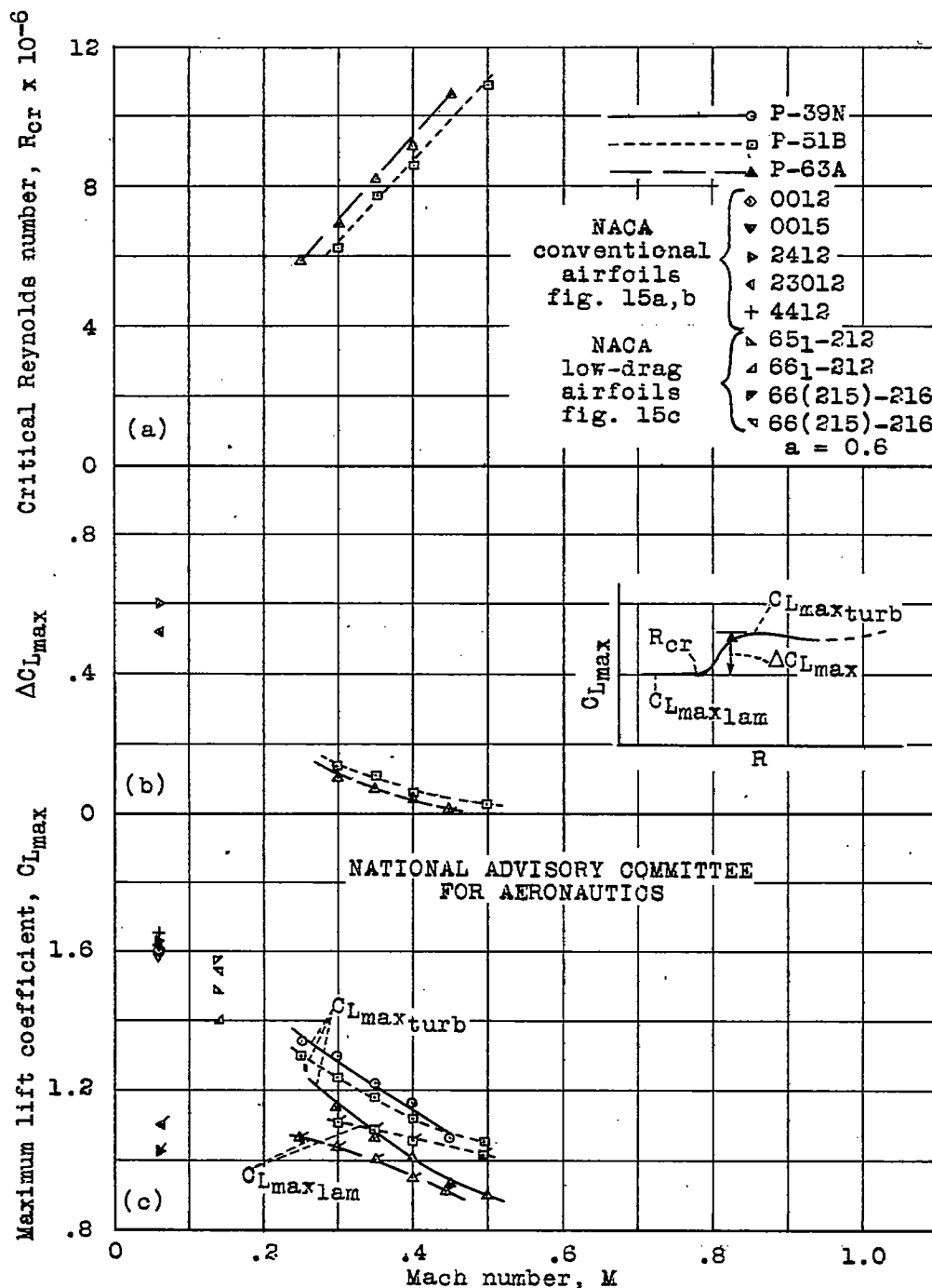


Figure 11.- Effect of Mach number on four parameters indicating the variation of maximum lift coefficient with Reynolds number.

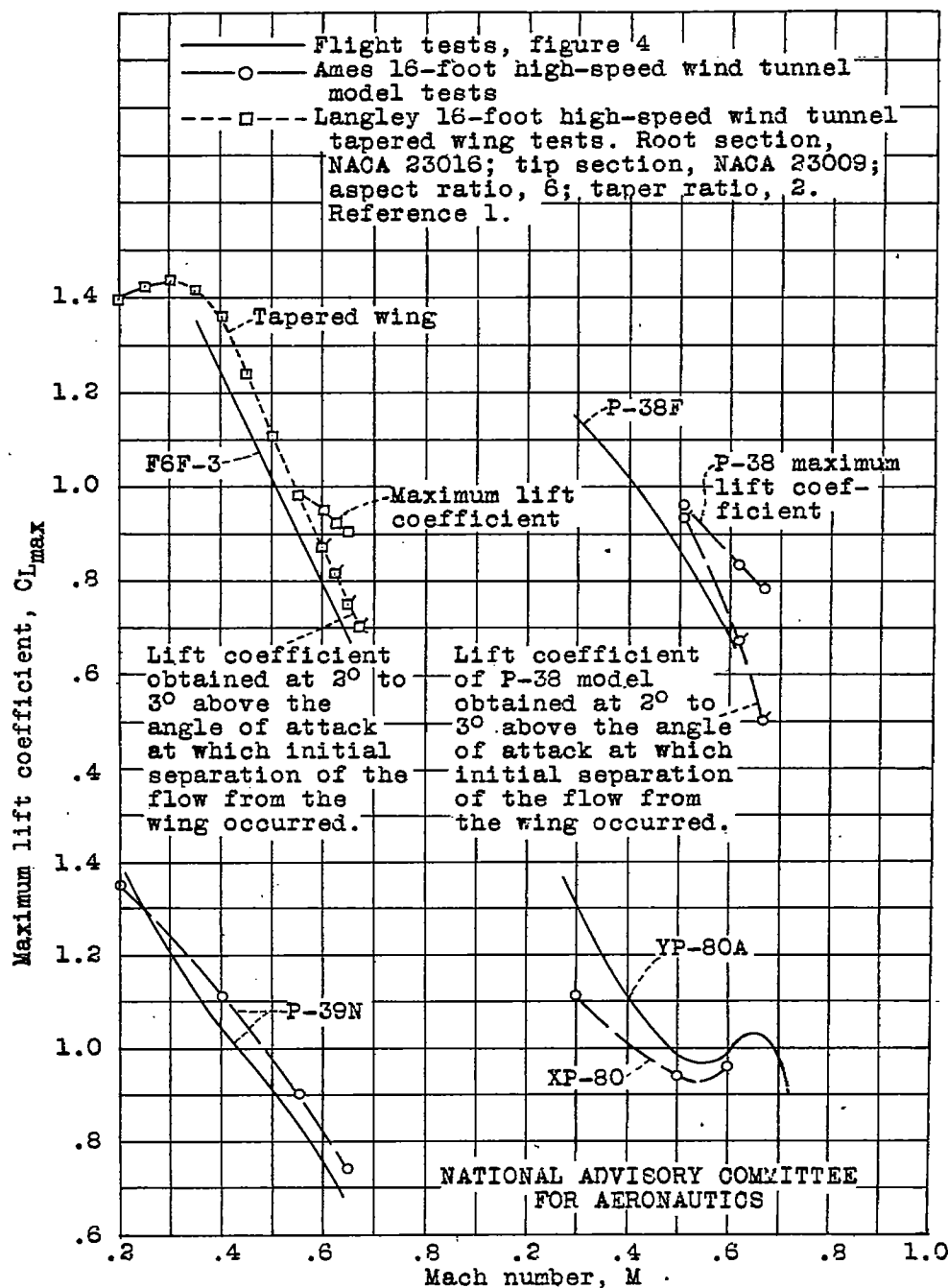


Figure 12.- Comparison of high-altitude flight data with wind-tunnel data showing the variation of maximum lift coefficient with Mach number.

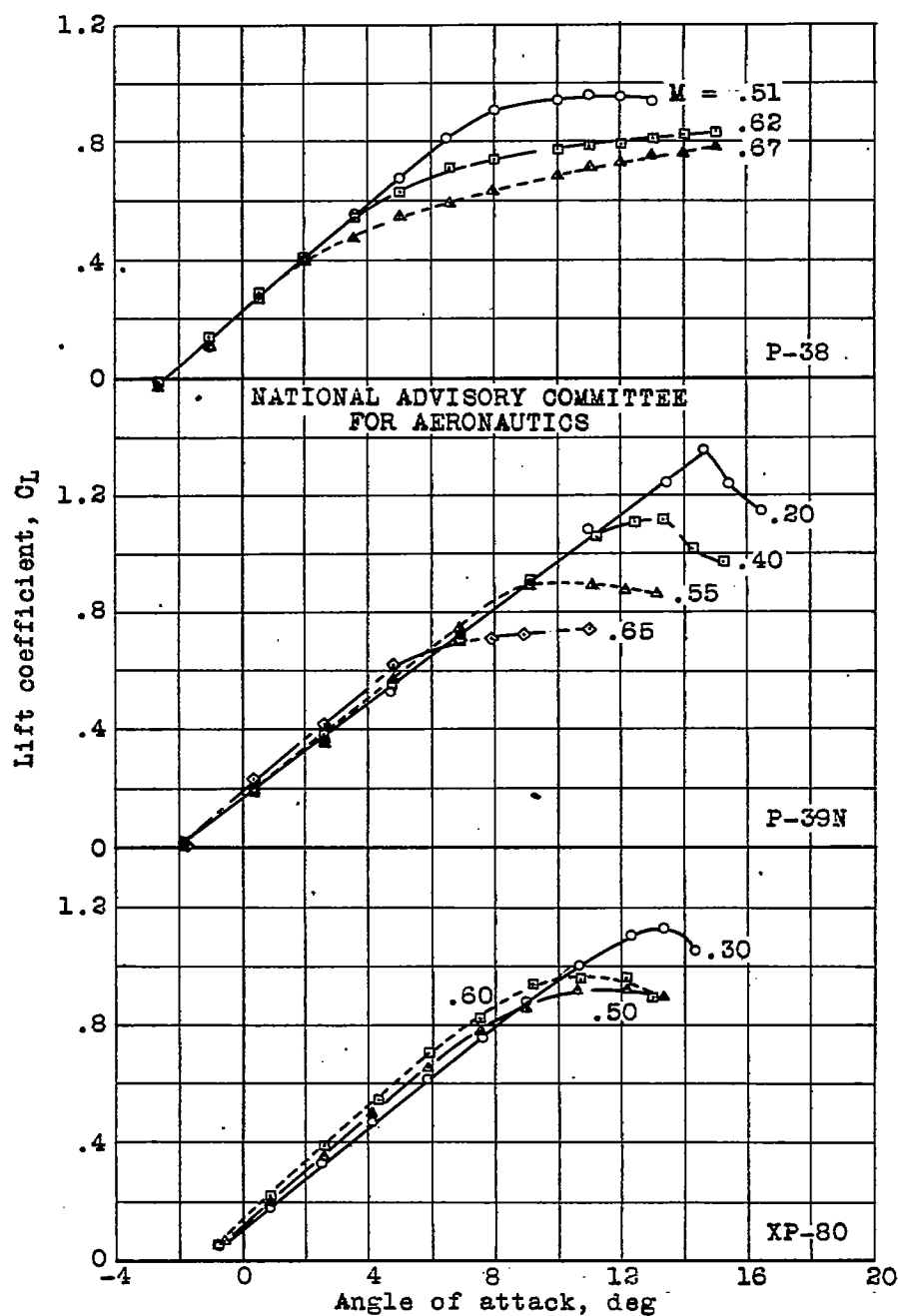


Figure 13.- Variation of lift coefficient with angle of attack at several Mach numbers for three models. Ames 16-foot high-speed wind tunnel.

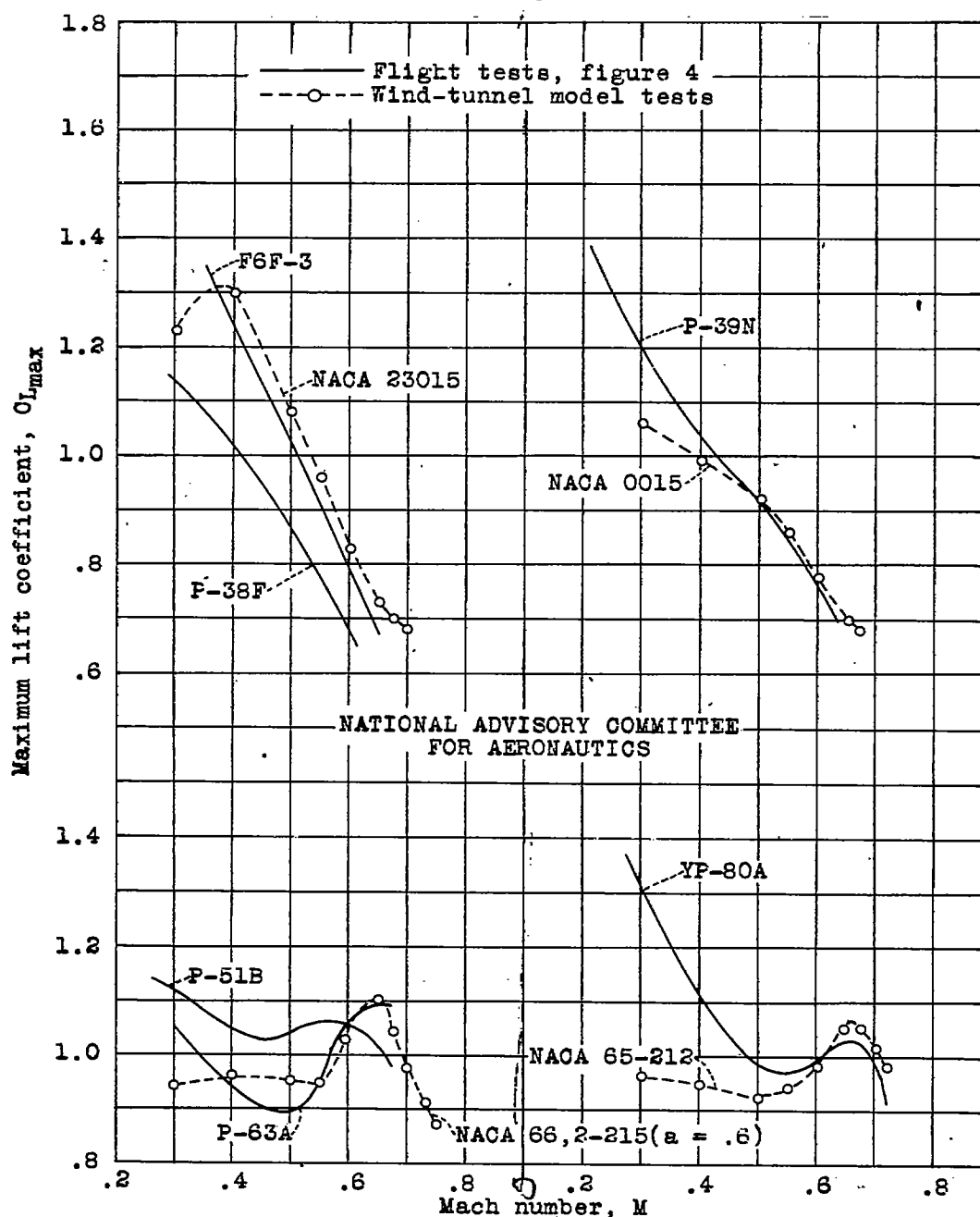


Figure 14.- Comparison of high-altitude flight data with Ames 1-by 3-1/2-foot high-speed wind-tunnel data showing the variation of maximum lift coefficient with Mach number.

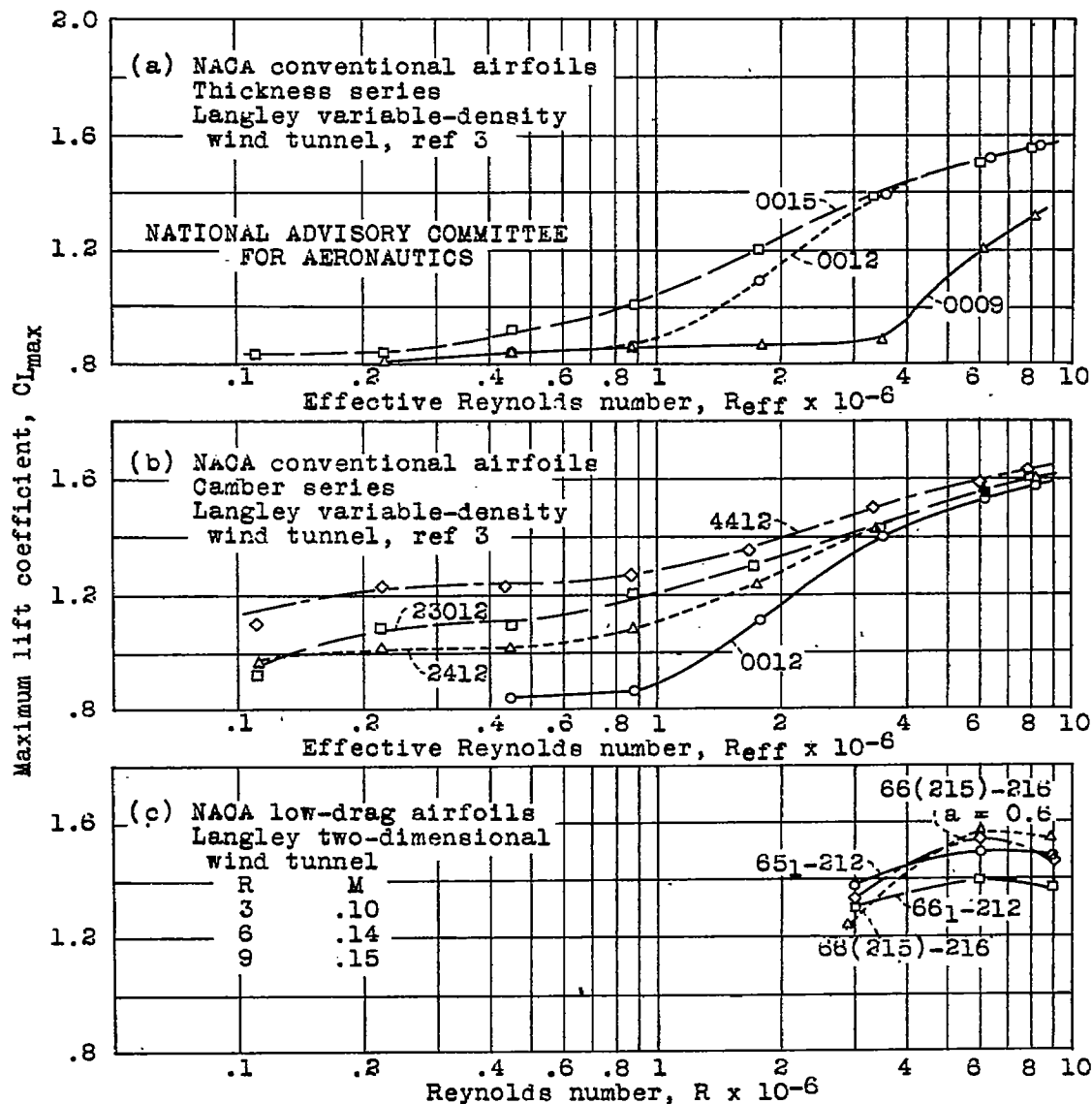


Figure 15.- Variation with Reynolds number of the maximum lift coefficients of several NACA conventional and low-drag airfoils.

NACA TM No. 1044

Fig. 16

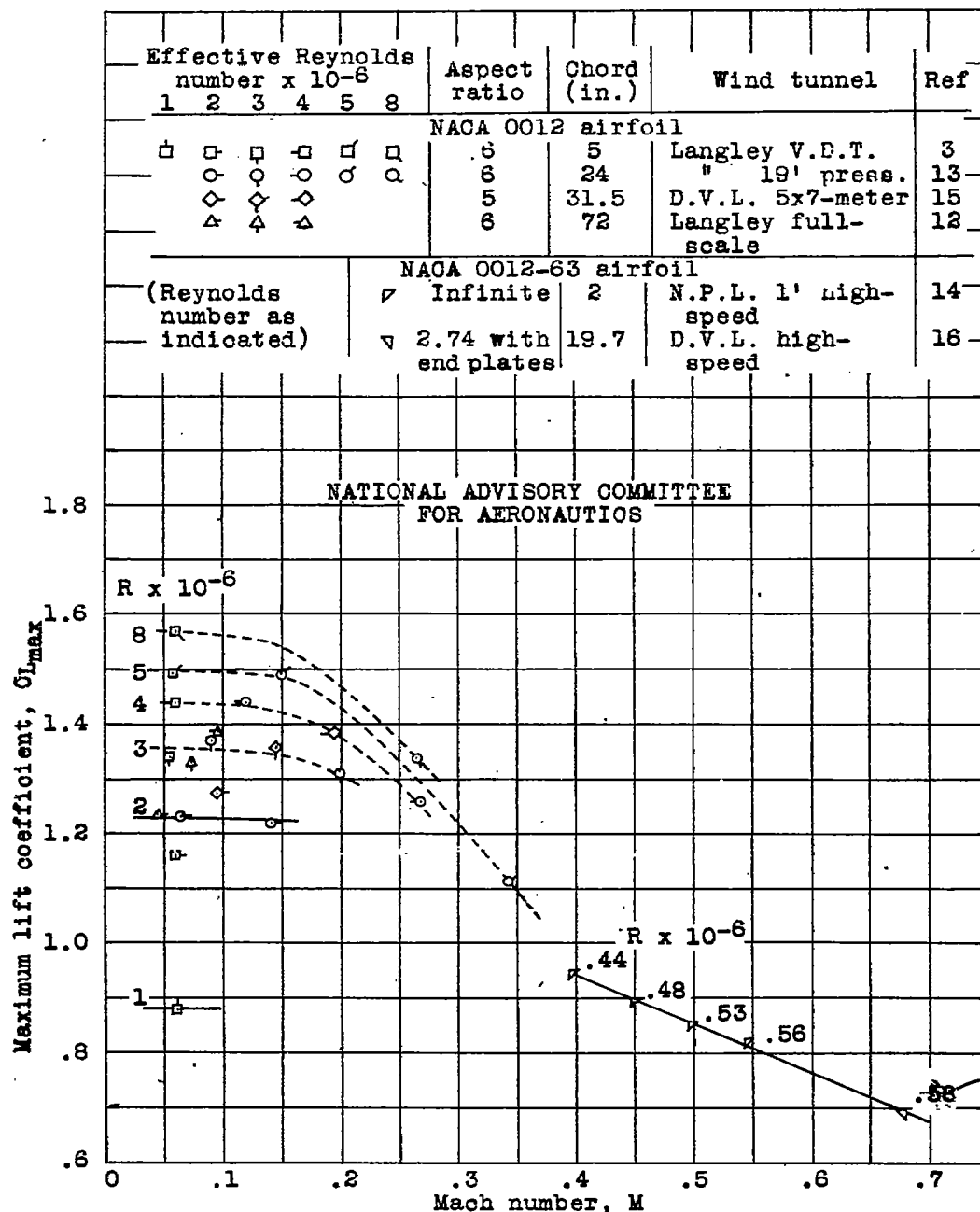


Figure 16.- Maximum lift coefficients of NACA 0012 and 0012-63 airfoils as measured in several wind tunnels.